CONTROL AND OPTIMIZATION OF VAPOR COMPRESSION CYCLES USING RECURSIVE LEAST SQUARES ESTIMATION

A Thesis

by

AVINASH RANI

Submitted to the Office of Graduate Studies of
Texas A&M University
in partial fulfillment of the requirements for the degree of

MASTER OF SCIENCE

August 2012

Major Subject: Mechanical Engineering

CONTROL AND OPTIMIZATION OF VAPOR COMPRESSION CYCLES USING RECURSIVE LEAST SQUARES ESTIMATION

A Thesis

by

AVINASH RANI

Submitted to the Office of Graduate Studies of
Texas A&M University
in partial fulfillment of the requirements for the degree of

MASTER OF SCIENCE

Approved by:

Chair of Committee,	Bryan Rasmussen
Committee Members,	Charles Culp
	Sivakumar Rathinam
Head of Department,	Jerald Caton

August 2012

Major Subject: Mechanical Engineering

ABSTRACT

Control and Optimization of Vapor Compression Cycles Using Recursive Least Squares Estimation. (August 2012)

Avinash Rani, B.E., Birla Institute of Technology

Chair of Advisory Committee: Dr. Bryan Rasmussen

Vapor compression cycles are the primary method by which refrigeration and air-conditioning systems operate, and thus constitute a significant portion of commercial and residential building energy consumption.

This thesis presents a data-driven approach to find the optimal operating conditions of a multi- evaporator system in order to minimize the energy consumption while meeting operational requirements such as constant cooling or constant evaporator outlet temperature. The experimental system used for controller evaluation is a custom built small-scale water chiller with three evaporators; each evaporator services a separate body of water, referred to as a cooling zone. The three evaporators are connected to a single condenser and variable speed compressor, and feature variable water flow and electronic expansion valves. The control problem lies in development of a control architecture that will minimize the energy consumed by the system without prior information about the system in the form of performance maps, or complex mathematical models.

The control architecture explored in this thesis relies on the data collected by sensors alone to formulate a function for the power consumption of the system in terms of controlled variables, namely, condenser and evaporator pressures, using recursive least squares estimation. This cost function is then minimized to attain optimal set points for the pressures which are fed to local controllers.

DEDICATION

To my parents

ACKNOWLEDGEMENTS

I would first like to thank Dr. Bryan Rasmussen for his guidance, patience and support throughout the development of this thesis. I would also like to thank Dr. Charles Culp and Dr. Sivakumar Rathinam for serving on my advisory committee.

Additionally, I would like to thank my colleagues at the Thermo-Fluids Controls Laboratory for the lively discussions and many laughs shared. I would specially like to thank Matt Elliott, for those insightful discussions and always being ready to lend a helping hand.

NOMENCLATURE

P_{ero}	Evaporator pressure
P_{cro}	Condenser pressure
Q_e	Evaporator cooling
T_{ewo}	Temperature of water at the evaporator outlet
T_{ewi}	Temperature of water at the evaporator inlet
T_{ero}	Temperature of refrigerant at the evaporator outlet
T_{eri}	Temperature of refrigerant at the evaporator inlet
$\dot{m}$	Mass flow rate
$\dot{W}$	Power
ICOP	Inverse Coefficient of Performance
EEV	Electronic Expansion Valve
WFV	Water Flow Valve

TABLE OF CONTENTS

LIST OF FIGURES

Page

LIST OF TABLES

Page

CHAPTER I

INTRODUCTION

BACKGROUND AND MOTIVATION

Vapor compression cycles are the basis on which refrigeration and air-conditioning units operate. They are used extensively in domestic, commercial and industrial applications, so they represent a high of energy consumption, and have high economic and environmental impact. In developed countries, they are responsible for roughly 30% of total energy consumption [1]. It is this large amount of energy being consumed by these processes that drives research in the fields of energy conservation and energy optimization. Control theory plays a very important role in realizing these goals. Traditional control techniques applied to vapor compression cycles include the use of simple electro-mechanical devices and on-off strategies. The advancement in technology in actuators and other components of the vapor compression cycles such as variable speed compressors, pumps, expansion valves etc, has allowed for more complex control strategies to be implemented, resulting in major energy savings. Typical control strategies involve maintaining state variables of interest, such as evaporator pressure, superheat, cooling etc, such that the energy consumption of the overall system in minimum. This thesis explores a new method of generating these optimal setpoints in a multi-evaporator vapor compression cycle.

This thesis follows the format of the *IEEE Transactions on Control Systems Technology*.

VAPOR COMPRESSION CYCLES

The equipment arrangement and interconnected piping for the ideal vapor compression system is shown in Figure 1.1. The four basic components of the system are the compressor, condenser, expansion valve and evaporator.

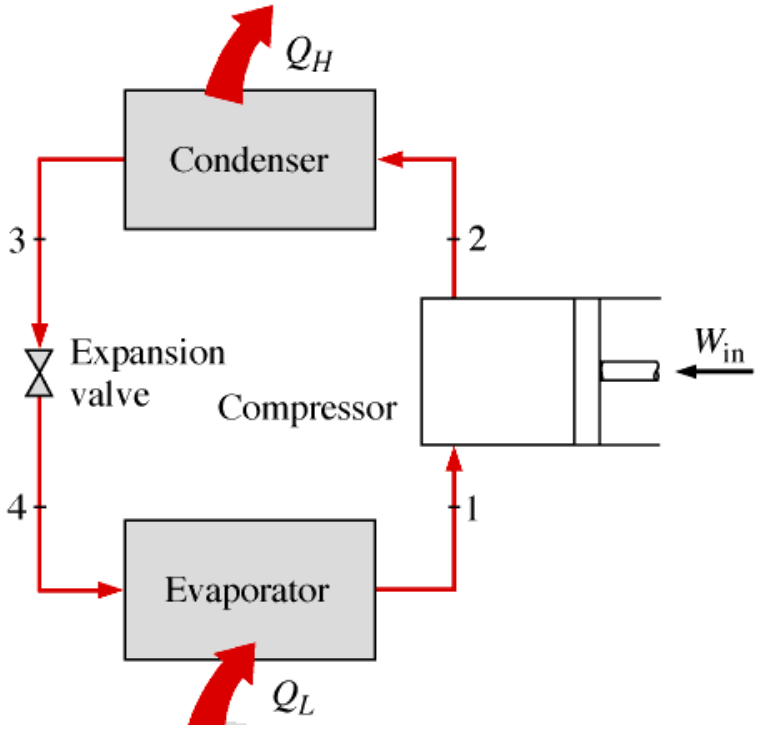

Figure 1.1: Vapor compression cycle from [2]

The processes that take place in the vapor compression cycle are are shown in Figure 1.2:

- The process 1-2 – Isotropic compression. The low temperature and low pressure super-heated vapor coming out of the evaporator is compressed to a high temperature and pressure at state 2.
- Process 2-3 – Isobaric condensation. The vapor at state 2 is condensed to high pressure state at 3 (saturated or sub-cooled liquid). Heat flows from the higher temperature refrigerant through the walls of the condenser to the cooling water.
- Process 3-4 – Isenthalpic expansion. The liquid refrigerant expands and cools down as it passes from high pressure to low pressure region through the expansion valve at state 4 (refrigerant is in two phase).
- Process 4-1 – Isobaric evaporation. The fluid at state 4 flows through the evaporator, where it absorbs heat from the circulating fluid, and vaporizes to vapor at state 1.

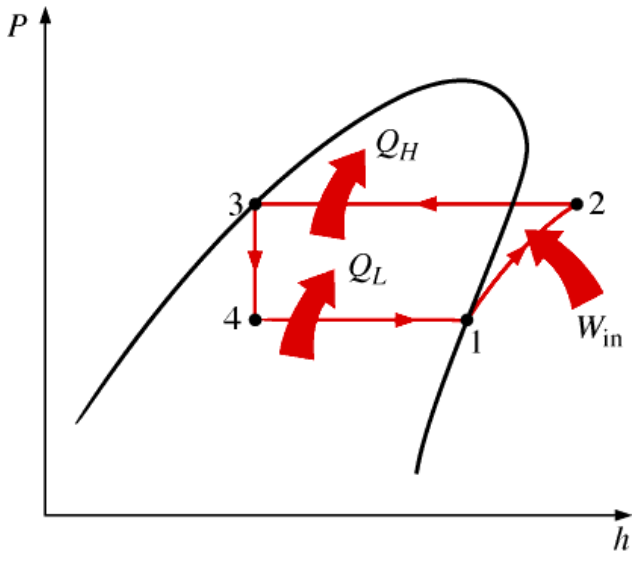

Figure 1.2: Pressure-Enthalpy diagram of a vapor compression cycle from [2]

Multi-evaporator refrigeration systems are used in installations such as supermarkets, food storage plants and residential complexes, where different zones have different cooling requirements. Depending on the applications and system requirements, various complex vapor compression systems can be built to serve a particular purpose. Multi-evaporator refrigeration systems can be classified [3] as shown in Figure 1.3 below. Note that in the case of expansion valves, there can be one EEV servicing multiple evaporators or every evaporator having its own individual EEV.

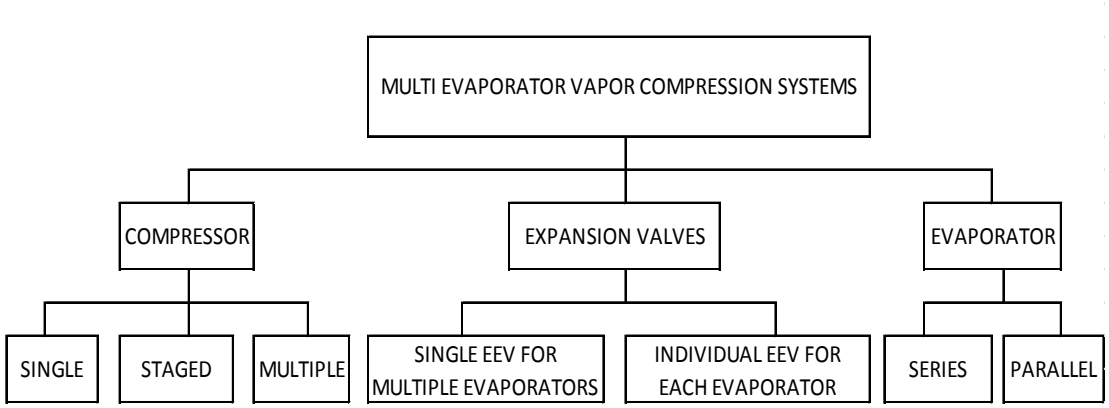

Figure 1.3: Classification of multi-evaporator vapor compression systems

LITERATURE REVIEW

In the last two decades, control theory has had immense success in terms of reducing over-all system operating cost of HVAC systems, ensuring thermal comfort, improving air quality, and generally making air-conditioning and refrigeration systems more efficient. Control functions applied to HVAC systems can broadly be divided into two categories: local control and supervisory control. Local control techniques are used to keep the refrigeration system running at predetermined setpoints, and may not be energy efficient or cost-effective where the overall system performance is concerned.

Supervisory control, on the other hand seeks to minimize or maximize an objective function pertaining to system performance in order to improve energy efficiency of the entire system by systematically seeking optimal operating conditions. Typical local control methods include application of Proportional-Integral-Derivative control, On/Off control, step control and modulating control, and all of these are effective control actuation schemes of local control loops in HVAC practice [4]. Gruhle and Isermann compared the performance of a PID controller favorably to that of a TEV in [5]. In addition, other single-input, single-output controllers have been implemented that use the EEV to control superheat. In [6], Outtagarts compared the use of PID with that of optimal qualitative regulation. Finn and Doyle compare PID performance with that of a TEV, and explore using adaptive PID control to improve performance [7]. Larsen, Thybo, and Rasmussen applied a nonlinear evaporator model and cascaded PID loops to the superheat control problem, where an outer loop calculated the necessary mass flow for a desired superheat setpoint, and fed this as a setpoint to an inner PID controller, which directly controlled the EEV [8]. Elliott [9] presented a global controller using model predictive control based approach to generate optimal setpoints for local controllers in order to balance goals of cooling zone temperature tracking with optimal energy consumption

Supervisory control consists of more complex optimal control methods that seek to maximize or minimize a real function by systematically choosing the values of variables within acceptable ranges. Some examples of supervisory control include:

MODEL BASED SUPERVISORY CONTROL METHODS

These methods use dynamic or static governing equations to construct models of vapor compression cycles to which control methods are applied. All the governing equations are derived from fundamental laws of energy, heat and mass transfer, flow balance etc. He, Liu, and Asada applied an advanced model-based control technique, Linear Quadratic Gaussian (LQG) control, in a multi-input, multi-output (MIMO) configuration to regulate superheat and evaporator temperature using a variable-speed compressor and EEV [10]. In [11] and [12], He and Asada developed a control architecture implementing a nonlinear observer to perform feedback linearization, allowing a PI controller to control compressor speed. In [13] Larsen developed a model based prediction of the steady state cost function gradient to drive the system towards optimal steady state operation.

PERFORMANCE MAP BASED SUPERVISORY CONTROL METHODS

Performance based supervisory control for chiller plants such as those studied by Hackner et al and Lau utilized component models to test and search for the minimum power consumption combination for each combination of the control variables. Sun and Reddy [14] showed that optimal control maps can be generated using detailed simulations. Yao et al [15] proposed a control strategy based on field tests over a significant range of settings and operating conditions. These methods require detailed simulations or experiments over a range of varied operating conditions for the targeted system, which makes it a cumbersome process for larger systems. But for smaller

systems, performance maps are a feasible and computationally inexpensive alternative to optimal control methods.

EMPIRICAL RELATIONSHIP BASED SUPERVISORY CONTROL METHODS

Polynomial regression or empirical relationships derived from data are the easiest way to construct a system model. These are data based models that utilize known and measured inputs and outputs from sensor data to formulate a control strategy. A few studies that use empirical relationship based models are discussed in the following pages.

Optimal control strategies for generating set points of controlled variables in the cooling plants have been studied by computer simulation by Ahn and Mitchell [16]. They developed a quadratic linear regression based equation for predicting the total cooling system power in terms of the controlled and uncontrolled variables using simulated data collected under different values of controlled and uncontrolled variables. The optimal set temperatures such as supply air temperature, chilled water temperature, and condenser water temperature, were determined such that energy consumption was minimized as uncontrolled variables, load, ambient wet bulb temperature, and sensible heat ratio were changed. The chilled water loop pump and cooling tower fan speeds were controlled by a PID controller such that the supply air and condenser water set temperatures reached the set points designated by the optimal supervisory controller.

Austin [17] used biquadratic polynomial models of chillers and cooling towers to optimize condenser-water temperature setpoints. Lu et al. [18] presented a series of system optimizations for building HVAC systems. The objective function for global

optimization was formulated based on mathematical models of the component systems. Power consumption of the chillers was formulated based on an empirical model, while power functions of the condenser and evaporator fans was modeled as a function of water flow rate.

Olson and Liebman [19] presented a mathematical programming approach to determine which available chiller plant equipment to use to meet a cooling load as well as operating temperatures for the water flows throughout the system. First, a mixed-integer, non-linear formulation of the problem was developed. A heuristic approach for handling the integer variables was then presented which allowed very good solutions to be obtained by solving a series of continuous problems using sequential quadratic programming (SQP). Finally, regression analysis of a large number of optimizations were presented which showed a linear trend that could be used to help guide the chilled water control system to make long term control decisions.

Empirical relationship based models are easy to implement, and computation time is low. However the robustness of such methods is an issue in practice, especially in cases where systems operate at a range not covered by training data. The primary disadvantage with optimal control strategies is that they are, in most cases, system specific applications and they lack generality. This is the problem that this research seeks to address. The following chapters present an algorithm that can be generalized for any vapor compression cycle, one that initially requires training data, but is able to adapt appropriately to changes in operating conditions, and to be able to generate optimal

setpoints and minimize energy consumption without having any *a priori* information about the system.

CHAPTER II

EXPERIMENTAL SYSTEM

The experimental system used for this research is a custom built three evaporator water chiller at the Thermo-Fluids Control Laboratory at the Texas A&M University. This chapter takes the reader over the construction of the system, with details on each component on the primary (refrigerant) loop and secondary (water side) loop. The primary loop components are first explained, followed by the secondary loop components. The sensors and actuators used in the system are described. Lastly, the data acquisition system, along with the software is described. The Experimental system is shown in Figure 2.1 below.

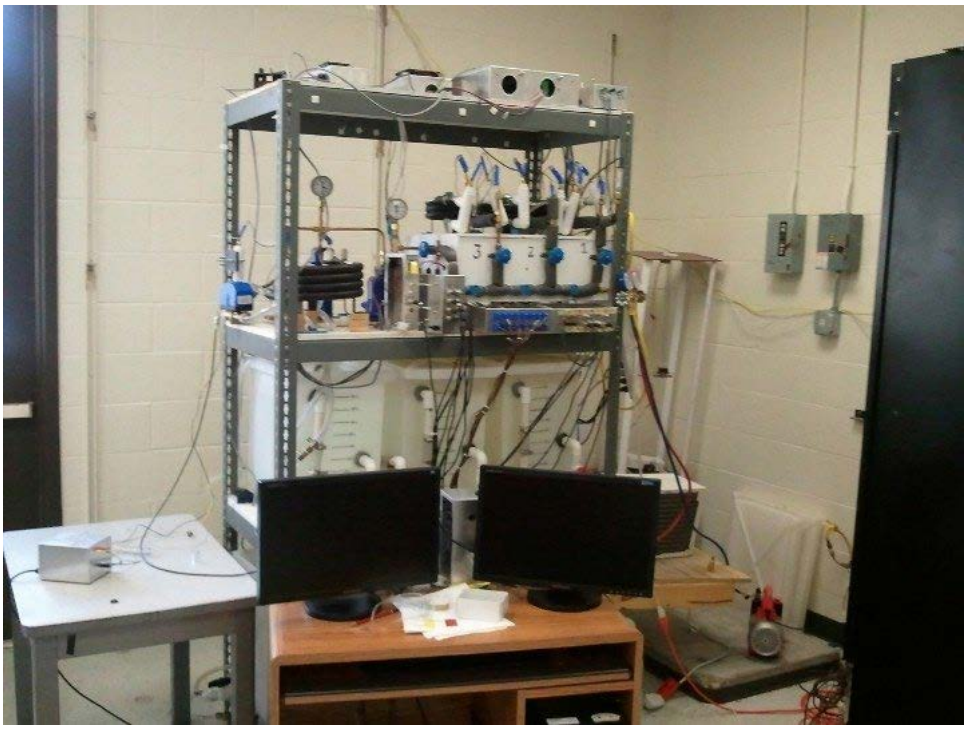

Figure 2.1: The experimental system

OVERVIEW

PRIMARY LOOP

The refrigerant side of the system is constructed using copper tubing. 1/4” tubes are used for lines carrying liquid refrigerant, while 3/8” tubes are used for lines carrying gaseous refrigerant or that in two-phase. A liquid receiver is installed between the condenser and expansion valves, to ensure that saturated liquid goes through the valves. Manual shutoff valves are installed at various points in the refrigerant flow loop in order to retain refrigerant in certain parts of the loop, while other parts are being worked on. There is a variable speed compressor with an accumulator to prevent liquid from entering the compressor. A schematic of the primary loop is shown in Figure 2.2 with all the components and their corresponding part numbers being detailed in Table 2.1. Table 2.3 describes the transducers used in the water chiller system and defines the sensor labels shown in Figure 2.2

SECONDARY LOOP

Water is used as the secondary fluid in the heat exchangers. Each of the heat exchangers has a water tank from where the water is fed and released into. The water is fed to the heat exchangers by means of water pumps. The water supply to the heat exchangers is isolated, and the water tanks represent cooling zones. This allows for simulations involving multiple cooling zones. A schematic of the secondary loop is shown in Figure 2.3 with the components tabulated in table 2.2. Table 2.3 describes the sensor labels shown in Figure 2.3.

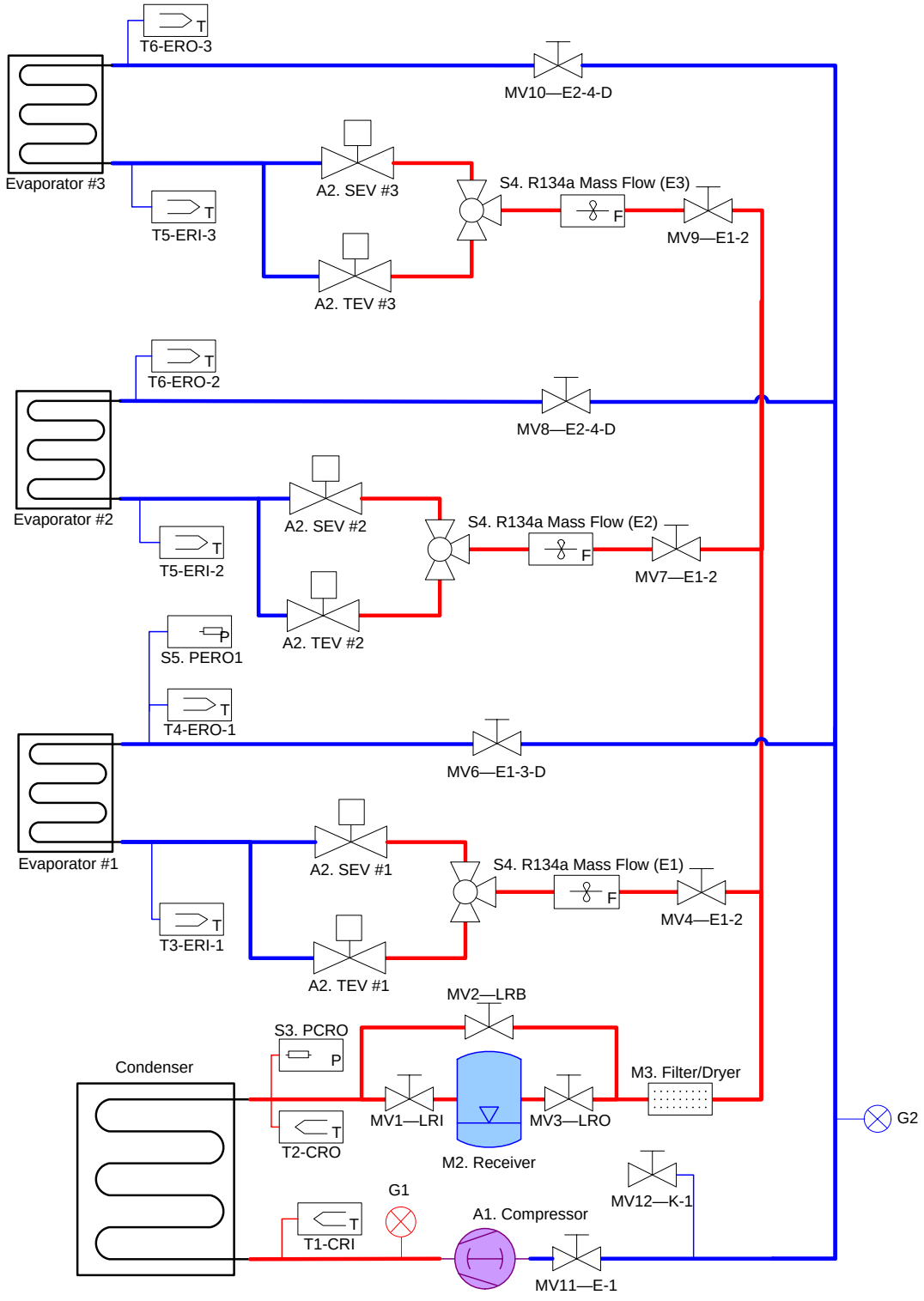

Figure 2.2: Primary loop schematic

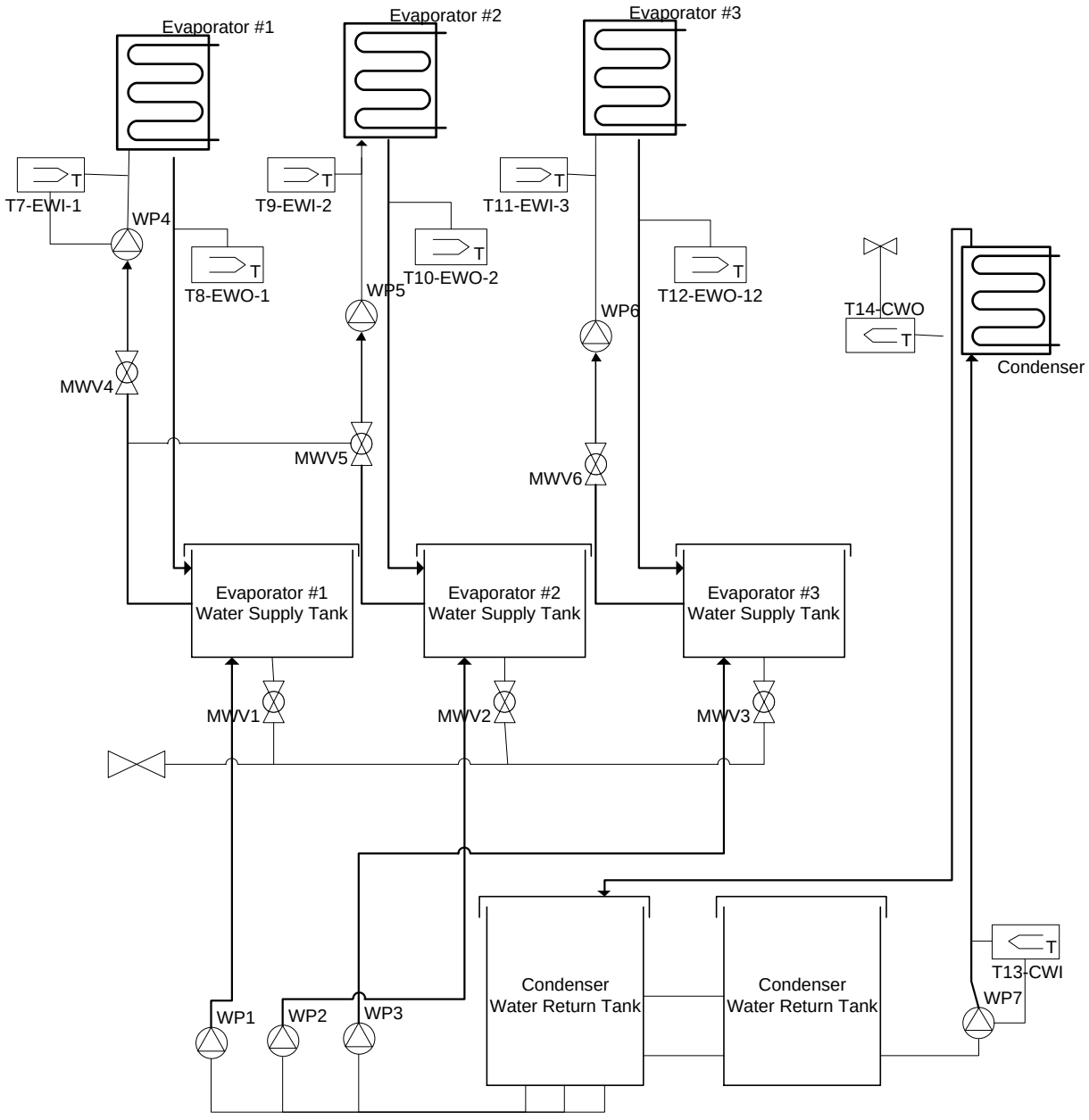

Figure 2.3: Secondary loop schematic

PRIMARY LOOP COMPONENTS

COMPRESSOR

The compressor installed on this system is a Masterflux make Sierra model scroll type variable speed compressor. The power supply is rated at 24/48 volt DC, and it is designed to run on R-134a refrigerant. The manufacturer provides a motor controller which accepts signals from the user to regulate compressor speed. The speed set point is controlled by a zero to five volt analog input, which in turn varies the compressor speed between 1800-6500 rpm. The controller also outputs a 0-5 volt tachometer pulse that indicates motor speed. The compressor capacity is rated at 1.5 tons of cooling. Figure 2.4 is a photo of the compressor.

Figure 2.4: Compressor

HEAT EXCHANGERS

The heat exchangers are helical coils, which utilize a 'tube-in-tube' design, manufactured by Packless industries. Water flows through the inner tubes while refrigerant flows through the annulus between the inner and outer tubes. Heat transfer is achieved with a counter-flow arrangement of water and refrigerant during condensing. The outer shell is made of stainless steel while the inner shell is made from cupro-nickel. The system has one condenser and three evaporators installed. The specifications of the condenser and evaporators are listed in table 2.1. A photo of the evaporators is shown in Figure 2.5

Figure 2.5: Evaporators

EXPANSION VALVES

The system has both thermostatic expansion valves and electronic expansion valves, for each evaporator. The EEV's are manufactured by Microstaq while the TXV's are manufactured by Sporlan. The specifications for the expansion valves are listed in table 2.1. Figure 2.6 is a photo of the EEV.

Figure 2.6: Expansion valve

Manual shutoff valves are also installed at various points in the primary loop. This allows one or more evaporators to be shut off, or for a section of the primary loop to be shut off, depending on requirements. Figure 2.7 is a photo of a manual shutoff valve.

Figure 2.7: Manual shutoff valve

LIQUID RECEIVER

A series S-8060 liquid receiver manufactured by Henry Technologies is installed at the end of the condenser. The purpose of a liquid receiver is to ensure that the refrigerant is at a saturated liquid state while entering the expansion valves. A photo of the liquid receiver is shown in Figure 2.8.

Figure 2.8: Refrigerant receiver

FILTER-DRIER

A filter/drier is installed after the receiver in order to protect the expansion valves. Figure 2.9 is a photo of the filter/drier.

Figure 2.9: Filter/drier

PRESSURE GAUGES

Pressure gauges are installed on the high and low pressure sides on the primary loop. The pressure gauges are manufactured by Omega. The high side pressure gauge has a range of 0-300 psi while the low pressure gauge has a range of 0-160 psi. Figure 2.10 is a photo of the low side pressure gauge.

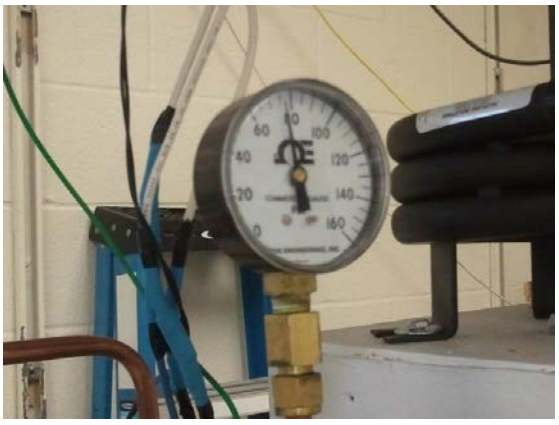

Figure 2.10: Pressure gauge

Table 2.1: Primary loop component specifications

Description	Qty	Manufacturer	Part Number	Notes	Schematic Reference
Thermal Expansion Valve (TXV)	3	Sporlan	SEI 0.5-10-S	R134a expansion	A2, A3, A4
Manual Shutoff Valve, 1/4"	8	Mueller	A14833	Refrigerant routing	MVx-xx-x
Manual Shutoff Valve, 1/4"	4	Mueller	14835	Refrigerant routing	MVx-xx-x
3-way Ball Valve, 3/8"	3	ValveWorx	536503	Auxilary valve selector	MV13-E2-6
Compressor	1	Masterflux	Sierra 03-0982Y3	-	A1
Condenser	1	Packless industries	COCX-2150-H	-	-
Evaporator	3	Packless industries	CHAX-3300-H	-	-
Sight Glass	1	Emerson	AMI 1FM2	1/4" female X male SAE	-
Venturi	1	Lambda Square	VU-0.5-0.148	1/2" size; 0.148" throat	M1
High Pressure Gage	1	Omega	PGC-25L-300	0-300 psig range	G1
Low Pressure Gage	1	Omega	PGC-25L-160	0-160 psig range	G2
Pressure Shutoff Switch	1	Ranco	012-1594-70	-	-
Silicon Expansion Valve (SEV)	3	Microstaq	SH09K1	R134a expansion	A5, A6,A7

SECONDARY LOOP COMPONENTS

WATER PUMPS

There are 7 water pumps in total, which help keep the water flowing through the secondary loop. There are 6 Swifttech MCP 350 variable flow water pumps that pump the water from the water tanks through the evaporators and back into the tanks. They have a flow rate of 117 gallons per hour (GPH), while the condenser is serviced by a Swifttech MCP 650 variable speed pump with a flow rate of 320 GPH. The water pumps are controlled using 4-20mA output signals from the DAQ computer. Since the pumps only respond to a change in voltage, a series of differential amplifier circuits are used in convert the output signals from the DAQ computer to voltage to the pumps. Figure 2.11 is a photo of the condenser water pump.

Figure 2.11: Condenser water pump

WATER FLOW VALVE

There is one electrically actuated water flow valve that is installed before the condenser. The actuator accepts a 4-20 mA signal from the user that opens and closes the valve accordingly. This valve is used to regulate the flow of water through the condenser. Figure 2.12 is a photo of the water flow valve.

Figure 2.12: Water flow valve

Table 2.2: Secondary loop component table

Description	Qty	Mfr	Part Number	Notes	Schematic Reference
Water Flow Valve (WFV)	1	Erie	APA23A000	water flow control	-
Transformer	1	Honeywell	AT72D-1683	24 VAC	-
Manual Water Valves	7	various		standard 3/4" PVC ball valves	MWVxx
Water Pumps	6	Swifttech	MCP 355	Evaporator water pumps	WPx
Water pump	1	Swifttech	MCP 650	Condenser water pump	WP7
Condenser Water Chiller	1	Haier	HWF05XC5T	5000 BTU/hr rating	-
Condenser Water Tanks	2	Tamco	6314	34 gallons	-
Evaporator Water Tanks	3	Tamco	6305	15 gallons	-

TRANSDUCERS

This section describes the transducers installed on the multi-evaporator system. The specifications of the transducers are tabulated in Table 2.3 below:

Table 2.3: Transducer specifications

Description	Qty	Mfr.	Part Number	Operating Range	Output Listed	Accuracy, +/-	Schematic Reference
Thermocouples	14	Omega	GTMQSS-062U-6	-270-400°C	TC	0.5 °C	Tx-xxx-x
Evaporator Pressure	1	Cole-Parmer	07356-03	0-160 psig	1-5 V	1.0%	Pero
Condenser Pressure		Cole-Parmer	07356-04	0-300 psig	1-5 V	1.0%	Pcro
Refrigerant Flow	3	McMillan	102-5-E-Q-B4-NIST	50-500 mL/min	0-5 V	3.0%	-
Compressor Current	1	CR Magnetics	CR5210	0-50 amps DC	0-5 V	1.0%	-
Tachometer	1	Masterflu x	-	1800-6500 RPM	0-2600 Hz	-	-

REFRIGERANT MASS FLOW

There are three McMillan Volumetric turbine-style flow meters installed at the end of the evaporators to measure the mass flow rate of the refrigerant. These transducers output a 0-5V signal to the DAQ board. Figure 2.13 is a photo of the refrigerant mass flow sensor.

Figure 2.13: Refrigerant mass flow sensor

PRESSURE

There are two pressure transducers installed on the system, both manufactured by Cole-Parmer. The first one, with a range of 0-300 psi is installed at the outlet of the condenser, while the second, with a range of 0-100 psi is installed at the outlet of the first evaporator. Both the transducers output a signal of 1-5 volts which is fed into the data acquisition boards. Figure 2.14 is a photo of the pressure transducer.

Figure 2.14: Pressure sensor

THERMOCOUPLES

Thermocouples are located at the inlet and outlet of the heat exchangers on both primary and secondary loops to measure the temperatures of the refrigerant and water during operation. The thermocouples are of Type T, with ungrounded sealed tips and pick up low noise. The thermocouples are arranged as shown in the figure below. The thermocouples are wired into a thermocouple terminal board which sends the signals to a PCI thermocouple board on the computer. Figure 2.15 is a photo of the thermocouples.

Figure 2.15: Thermocouples

CURRENT TRANSDUCER

The current is measured by a Hall Effect sensor to measure the DC current passing through the wire to the compressor. It is manufactured by CR Magnetics. The output of 0-5 volts is proportional to the current passing through the wires.

TACHOMETER

The compressor motor control outputs a 0-5V tachometer pulse that indicates motor speed. The frequency of the pulse is proportional to the motor speed.

DATA ACQUISITION

The data acquisition (DAQ) system is centered around four on-board DAQ boards installed on a personal computer (PC). Temperature measurements are performed using the type T thermocouples detailed earlier and recorded and logged using a Measurement Computing thermocouple board, model PCI-DAS-TC. Analog output signals to control compressor speed, valve positions, et cetera, are output by a Measurement Computing PCI-DDA-08 board. Sensor measurements are logged using a pair of National Instruments E-Series boards, model number E-6023. These boards have eight channels when connected in differential mode. They also have up to eight channels of digital output and two channels of analog output each.

SOFTWARE

The data logging and control functions are performed with WinCon 5.0, a software package by Quanser that provides a convenient interface with MatLab and Simulink. A Simulink model is created and compiled into a program that WinCon executes in real time. Parameters such as gains and analog inputs to the actuators can be changed in real time. Drivers for the thermocouple board and the analog output board were developed by researchers at the University of Illinois at Urbana-Champaign; these drivers were modified and implemented on the DAQ computer.

CHAPTER III

DYNAMIC ANALYSIS OF WATER CHILLER SYSTEM

The first step to designing any control strategy is to study the system behavior and effects of various inputs to the outputs. This is especially important with system as complex as a refrigeration or air-conditioning system, where there are a very large number of variables, and change in any one input parameter or a combination of input parameters brings about a change in an output parameter, thus making it necessary to understand the relationships between control inputs and system outputs. The idea is to identify input-output pairs, so as to use an input which has the maximum subsequent effect on an output when designing controllers. This chapter deals with the study of the dynamic relationships of a few important parameters with by using system identification methods. The analysis was done using the system identification toolbox in MATLAB [20].

SYSTEM IDENTIFICATION THEORY

System identification is defined as the use of statistical methods to build mathematical models of dynamic systems from measured data. There are three types of identification methods:

- White-box models – these are models that are derived from first principles. These models are most handy in lower order systems, but in most real-world problems, such models will be overly complex, and possibly even impossible to obtain in a reasonable time frame

- Grey box models – these models are based on both insight into the system and experimental data.
- Black box model – these are the models in which no prior knowledge of the system is required. There are purely based on experimental data. The model identified for this particular system is of this type.

In order to investigate the relationships between input output pairs, linear state space models was derived using system identification techniques. The system identification toolbox was used to construct linear state space models using the Prediction Error Method (PEM). The models developed are of the form:

$$x(k+1) = Ax(k) + Bu(k) \tag{1}$$

$$y(k) = Cx(k) + Du(k) + e(k) \tag{2}$$

$$x(0) = x_0 \tag{3}$$

PEM is a basic and very widely used identification method. It minimizes the cost function, which is defined as follows for a scalar input:

$$V_n = \Sigma_{t=1}^{n} e^2(t) \tag{4}$$

where *e* is the error between the model output and the supplied experimental data.

For black box models, PEM estimates an initial model and then varies the parameter values along a direction towards the minimum of the cost function. The PEM algorithm first makes an initial guess using the N4SID subspace algorithm and the refines the prediction error fit by minimizing a quadratic error prediction error [21]. More information on system identification can be found in [22]. The point of this exercise was

to determine the relationship between evaporator superheat, pressure and cooling to compressor RPM, EEV opening and water pump speed, not necessarily in that order. The system was operated over a range of operating conditions, in order to acquire data to build the models. This data was then processed and filtered in order to smoothen out transients and minimize the effect of sensor noise. Since the values for individual parameters may be of different scales, the data was normalized to reduce errors induced due to bad scaling. Normalization was done by subtracting the value of data at every instant from the maximum value in the data set and then dividing by the difference between maximum and minimum values, so that the value of every data point would be between 0 and 1 for the data sets of interest, with 1 being the reference value for the maximum and 0 being reference for the minimum. Figure 3.1 is a block diagram showing possible input/output pairs.

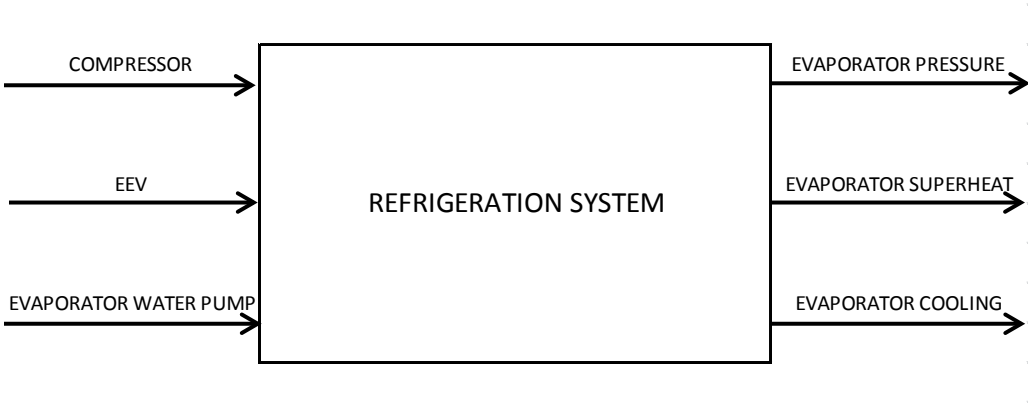

Figure 3.1: Block diagram with possible input/output pairs

The data is imported to the system identification toolbox in MATLAB. The procedure for identifying models requires two sets of data: the first set is used to create the model,

and the second set is used to validate it. Figure 3.2 below illustrates the procedure. The compressor speed is given as the input to the system and the evaporator is the output. The 'model creation' section is used to create models of any order that we specify. In this case, 1st to 4th order models were created for each input-output pair.

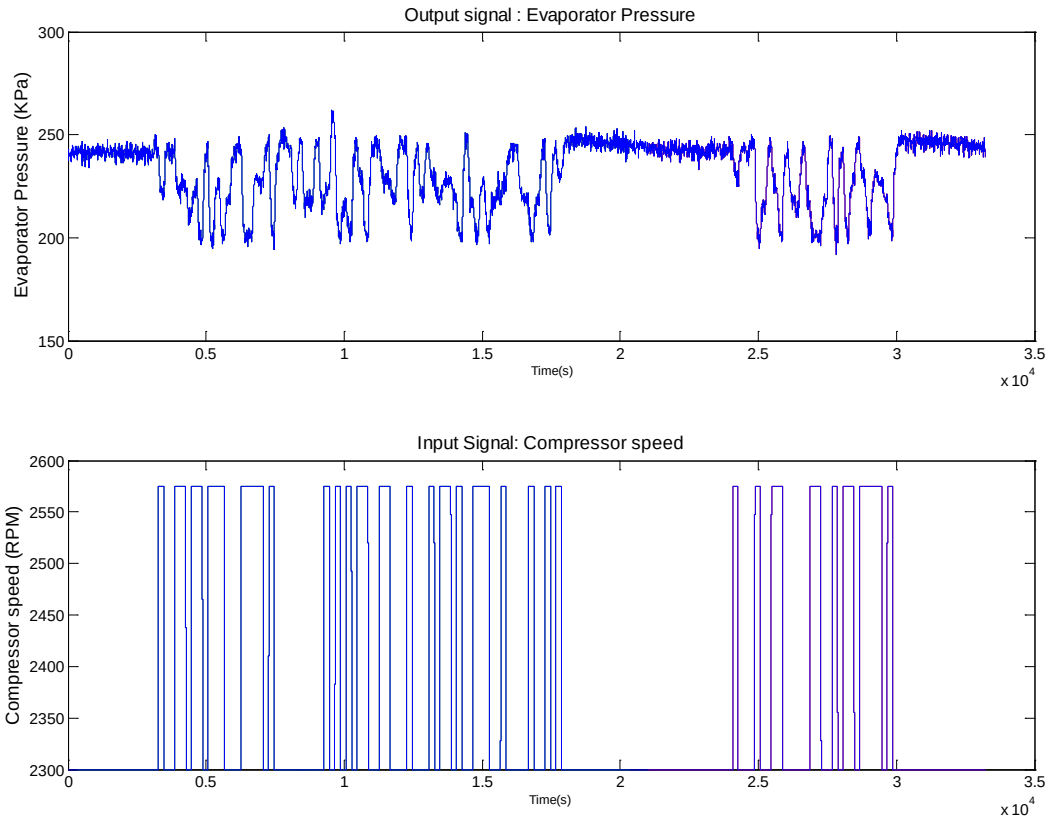

Figure 3.2: System Identification example data set

The program then calculates a quality of fit, which is a comparison between the output of the model against the measured data. The quality is a percentage value. This was done

for various combinations of input-output pairs. The quality of fit determined for each of the models is given in the table below:

Table 3.1: Quality of fit for each input-output pair

	ORDER	% FIT
RPM to Evaporator pressure	2	79.12%
	3	81.36%
	4	81.4%
Water pump to cooling	2	37.97%
	3	66.17%
	4	66.21%
EEV to superheat	2	81.68%
	3	82.54%
	4	83.39%

Once this is done, we have to select the model to be used for dynamic analysis. The ideal model would be one of a lower order and higher percentage of fit. For example, in the above table, we can see that 2^{nd} to 4^{th} order models for compressor RPM to evaporator pressure have similar quality of fit. One can choose any of the three, but it is advisable to choose the second order model, because higher, complex models do not yield significantly better results. In the case of WFV to cooling, we would choose the 3^{rd} order model over the 2^{nd} order one, just because the quality of fit is almost double. Once the state space models were selected, frequency response plots were generated for each of these models.

FREQUENCY RESPONSE OF EXPERIMENTAL SYSTEM

The data used for system identification was also used to determine the relationship between different input-output pairs, in order to determine the best actuators to be used to control the different output parameters. The data was first normalized to account for the differences in scales and units. Figure 3.3 shows the frequency response of the three outputs, Evaporator Pressure (Pero), Evaporator superheat (T_{SH}) and Evaporator Cooling (Q) to a step in compressor speed. Figure 3.3 shows that compressor RPM has a significant effect on evaporator superheat, but has the strongest effect on evaporator pressure

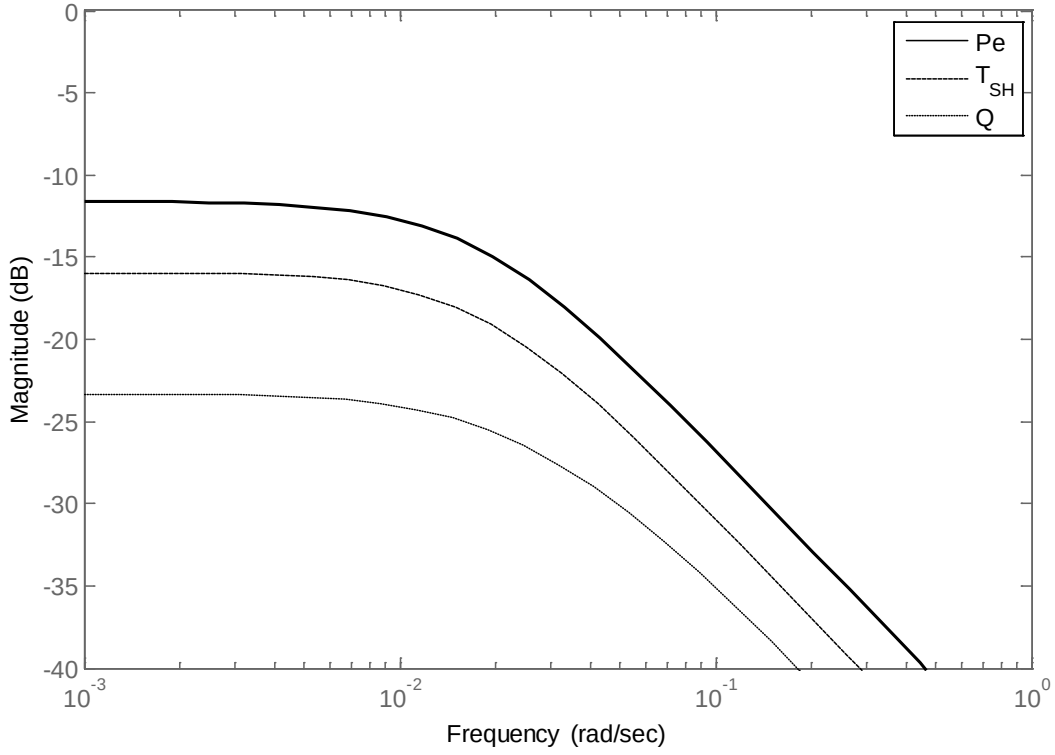

Figure 3.3: Normalized frequency response of various outputs to compressor speed

Figure 3.4 shows the effect of the water mass flow on the three outputs. The water mass flow is increased by increasing the speed of the water pump. Though its effect is the strongest on the superheat, it also results in increase in cooling.

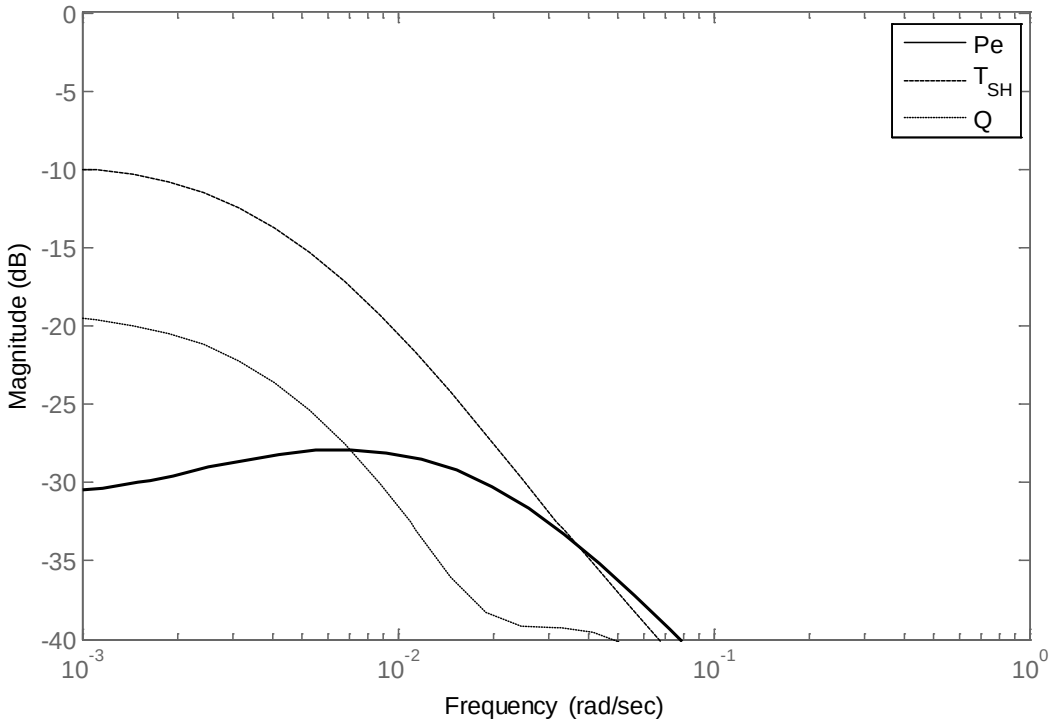

Figure 3.4: Normalized frequency response of various outputs to evaporator water pump speed

Figure 3.5 shows the frequency response of the three outputs to a step in the EEV. The EEV traditionally has a strong effect on both the evaporator pressure and superheat. The EEV also has a strong effect on the cooling, the reason being, that with an increase in the opening of the EEV, more refrigerant flows through the evaporator. This in turn results in an increase in cooling.

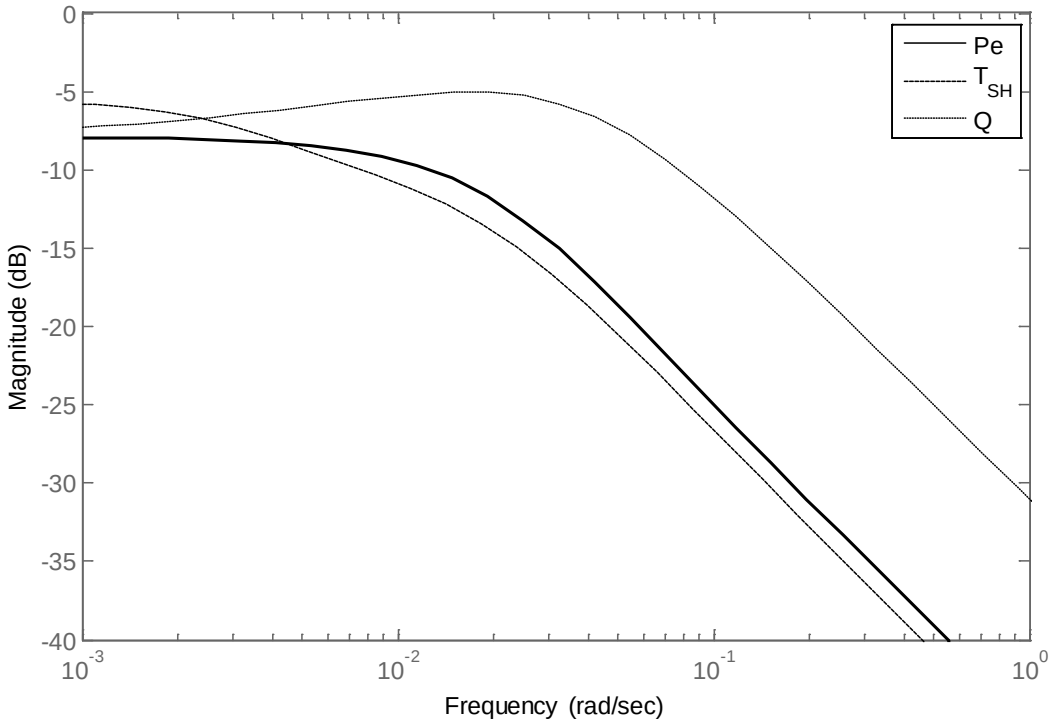

Figure 3.5: Normalized frequency response of various outputs to EEV opening

The frequency response plots show that there is a lot of dynamic coupling between the inputs and outputs. In practice, when the compressor RPM is stepped up, this brings about and immediate decrease in the evaporator pressure, as well as an increase in superheat and cooling. The same goes with the EEV's too. An increase or decrease in EEV opening brings about a change in each of the outputs.

CHAPTER IV

RECURSIVE LEAST SQUARES THEORY

Recursive least squares is an identification algorithm that is most frequently used when parameters are to be identified from recurring (real time) data [23]. This section deals with a background on the theory of Recursive least squares and how it is applied in this research.

Let a single linear algebraic equation at time 't' be written as

$$a_1x_1(t)+ a_2x_2(t)+....+ a_nx_n(t) = b(t) \tag{5}$$

where $a_ix_i(t)(i = 1,2,\ldots,n)$ and b(t) are known measurement data, and $x_i(t)$ $(i = 1,2\ldots,n)$ are coefficients that need to be determined. Evaluating the above equation at times $t_1,t_2,\ldots,t_m$, and writing the equations for each of those data points as a set of linear equations in matrix form, we have

$$X_0A_0 = B_0 \tag{6}$$

where, the entries of X_0 are given by $x_{ij} = x_i(t_j)$, (I = 1,2,…,n, and j = 1,2…,m), and the entries of A_0 are given by a_j (j = 1,2,…,n). Assuming that the matrix X_0 is full rank, the least squares solution to equation (2) is given by

$$A_o = (X_0^TX_0)^{-1}X_0^TB_0 \tag{7}$$

Now, let at some instant of time t_{m+1} the new data arrives, the new equation would be

$$a_1x_{m+1}(t_{m+1}) + a_2x_{m+1}(t_{m+1}) +....+ a_nx_{m+1}(t_{m+1}) = b(t_{m+1}) \tag{8}$$

which, written in matrix form would be

$$X_{new}A_{new} = B_{new} \tag{9}$$

The new equation can be added to the bottom of the original set of equations, to obtain the over-determined set of equations, as show below

$$X_{m+1}A_{m+1} = B_{m+1}, \tag{10}$$

where,

$$X_{m+1} = \begin{bmatrix} X_0 \\ X_{new} \end{bmatrix}, B_{m+1} = \begin{bmatrix} B_0 \\ B_{new} \end{bmatrix} \tag{11}$$

The solution to (11) is given by

$$A_{m+1} = (X_{m+1}{}^T X_{m+1})^{-1} X_{m+1}{}^T B_{m+1} \tag{12}$$

This means that the new solution for the coefficients for the equation would be calculated from scratch, and the original solution was not utilized in obtaining the new solution. This is a very inefficient method of solving the least squares problem, because the inverses are calculated again, requiring a large number of calculations which may not be necessary in the first place. Recursive least squares is a method by which the original solution is utilized in arriving at the new solution, by constantly updating itself as the new data keeps coming in. this method is robust as well as efficient.

The recursive least squares method introduces a correction factor, 'K', which is added to the original solution A_0. For example, for an instant $t = t_{m+1}$, the recursive least squares solution will be

$$A_{m+1} = A_m + K(B_{m+1} - A_m X_{m+1}) \tag{13}$$

where,

$$K = \frac{1}{1+a^T(A_0^T A_0)^{-1}a}(A_0^T A_0)^{-1}a \quad (14)$$

Let $P_0 = (A_0^T A_0)^{-1}$. The recursive least squares algorithm can now be written as:

$$A_{m+1} = A_m + K(B_{m+1} - A_m X_{m+1}) \quad (15)$$

$$K_{m+1} = \frac{1}{1+a^T P_0 a} P_m a \quad (16)$$

$$P_{m+1} = [I-Ka]P_m \quad (17)$$

The update of A_{m+1} is therefore a vector multiplied by the error $B_{m+1} - A_m X_{m+1}$ associated with the new equation using the original A_m. the matrix P_m is updated in the next iteration.

APPLICATION OF RECURSIVE LEAST SQUARES ALGORITHM

This section deals with the application of the theory described in the previous section to develop a recursive polynomial for power consumption as a function of evaporator and condenser pressures. The total power consumed by the system can be written as the sum of the power consumed by the compressor and water pumps servicing the evaporators and condenser. The sections below will give a brief description as to how these functions are constructed.

CONDENSER AND EVAPORATOR PUMP POWER FUNCTIONS

The power consumed by the pumps supplying water to the condenser and the evaporators was approximated as a function of their RPM. The relationship between power consumed and pump rotor speed is calculated from the following relationship:

$$\text{Power} = f(n^3) \quad (18)$$

where ‘n’ is the speed of the rotor in revolutions per minute.

The pumps are controlled by varying the voltage between 7.5 – 12 V. This in turn is done by changing the signals from the DAQ board. A differential amplifier circuit is used to change the signals given out from the DAQ board (4-20 mA) to the appropriate voltage required to run the pumps at variable speed. Tests were then run to identify the relationship between the signal given as input to the computer and the corresponding speed the pump was running at.

The following plot depicts the relationship between pump speed and DAQ signal:

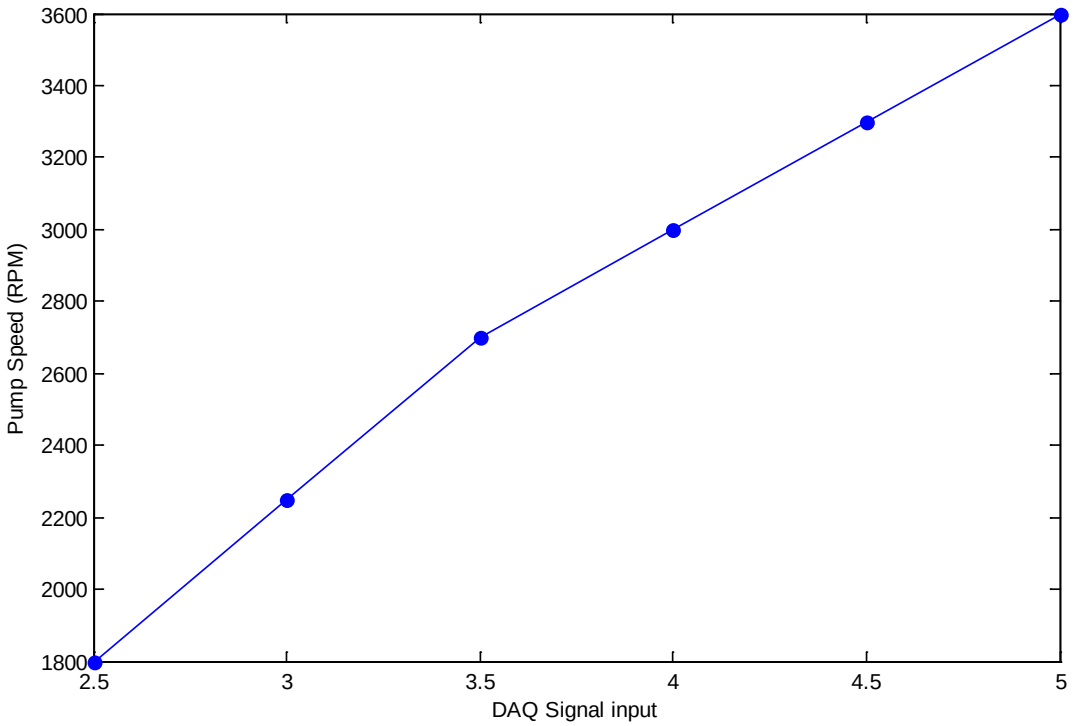

Figure 4.1: Relationship between DAQ signal and pump speed

A similar test was run for the condenser pump. The power function was finally formulated by using the equation:

$$\text{Power} = \alpha n^3 \tag{19}$$

where α is a proportionality constant. The power curve for the condenser pump is shown in Figure 4.2

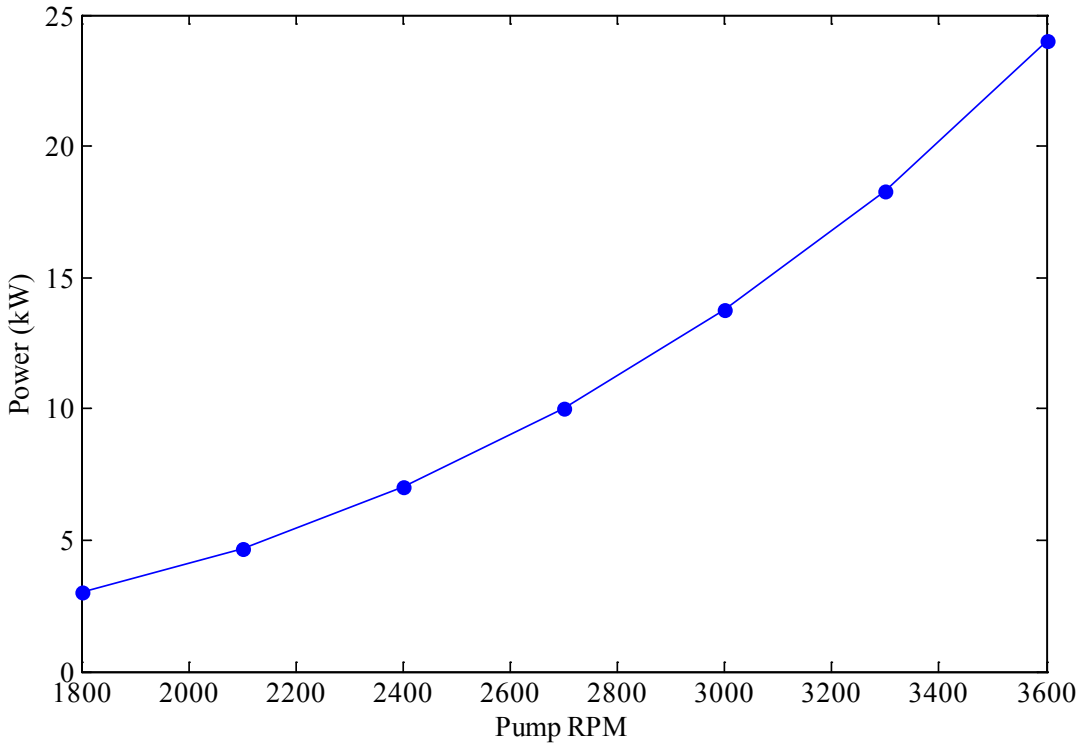

Figure 4.2: Power vs RPM curve for water pump

The power consumed by the compressor is measured by the current transducer. This signal (Amps) multiplied by the voltage gives us the power consumed (kW) at that

instant. So the total power consumed by the compressor and pumps can be summed up to be:

$$\text{Total Power} = \text{Power}_{\text{Compressor}} + \text{Power}_{\text{Condenser pump}} + \text{Power}_{\text{Evaporator pumps}} \quad (20)$$

EVAPORATOR COOLING CALCULATION

The cooling is determined by calculating the heat rejected in the water side of the evaporator. Thus this negates the requirement to install expensive refrigerant mass flow sensors in order to calculate cooling. Cooling is determined from the formula:

$$\dot{Q} = \dot{m}_{water} C_p (T_{ewi} - T_{ewo}) \quad (21)$$

The mass flow rate of water is calculated from an empirical relationship between the pump RPM and volumetric flow rate. This data is published by some pump manufacturers, although for the pumps hooked up to this system, this relationship had to be determined experimentally.

Figure 4.2 shows the relationship between the mass flow rate of water and the pump output to the voltage given to the pump, which is directly proportional to the pump speed.

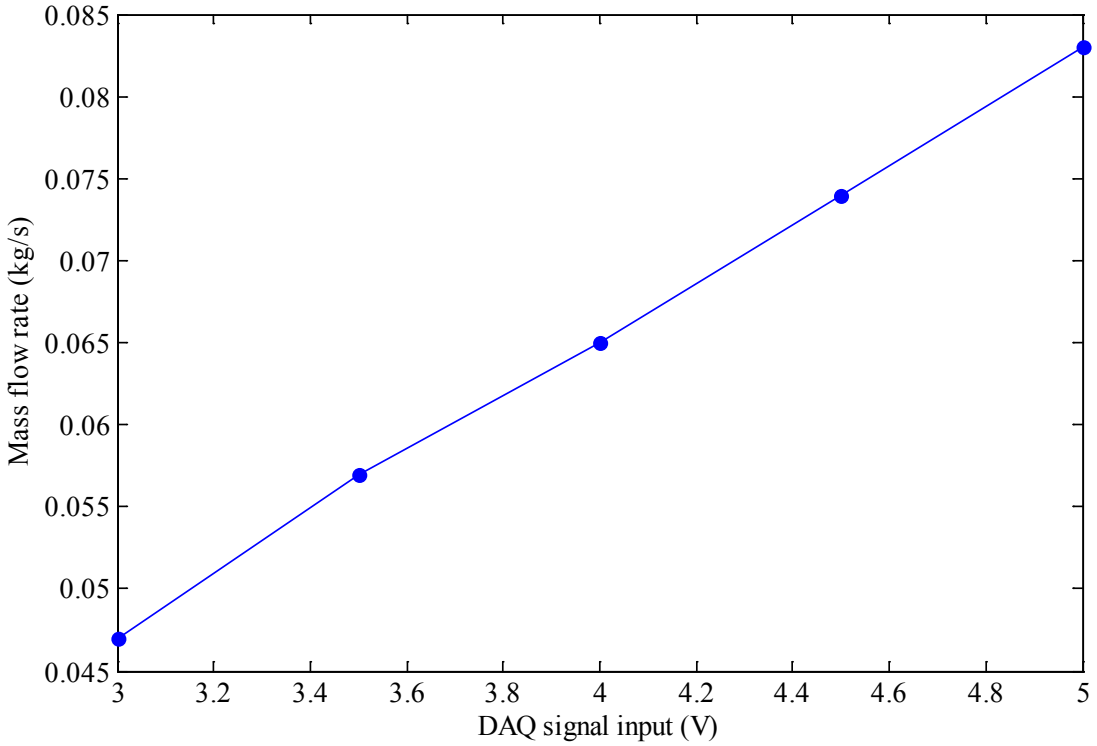

Figure 4.3: Relationship between input signal to water pump and mass flow rate at output

The cooling determined from this model was then compared with the cooling calculated from the refrigerant side calculations. Figure 4.3 shows the results of a test run as a check. The two values are almost equal. Figure 4.4 plots the error between the measured values (refrigerant side) and calculated values (water side). The water side calculations are used to calculate cooling in the evaporators for the experiments done in this thesis. The cooling in the refrigerant side is calculated by using equation (22)

$$\dot{Q} = \dot{m}_{ref}(h_{en,o} - h_{en,i}) \tag{22}$$

where,

$\dot{Q}$ = Cooling in the evaporator, kW

$\dot{m}_{ref}$= Maas flow of refrigerant 134a in the evaporator, kg/sec

$h_{en,o}$ = Enthalpy of R134a at evaporator exit, kJ/kg

$h_{en,i}$= Enthalpy of R134a at evaporator inlet, kJ/kg

A test was run to determine whether the cooling calculated from the water side is the same as that calculated from the refrigerant side. The compressor was switched on, and allowed to run at a constant speed. The cooling from both equations 21 and 22 was calculated and plotted. There was some discrepancy at the start because heat has to transfer through the walls of the heat exchanger which are cold, which causes a lag between the heat lost by the refrigerant and the heat gained by the water, but upon reaching steady state the error reduced to +/- 0.2%.

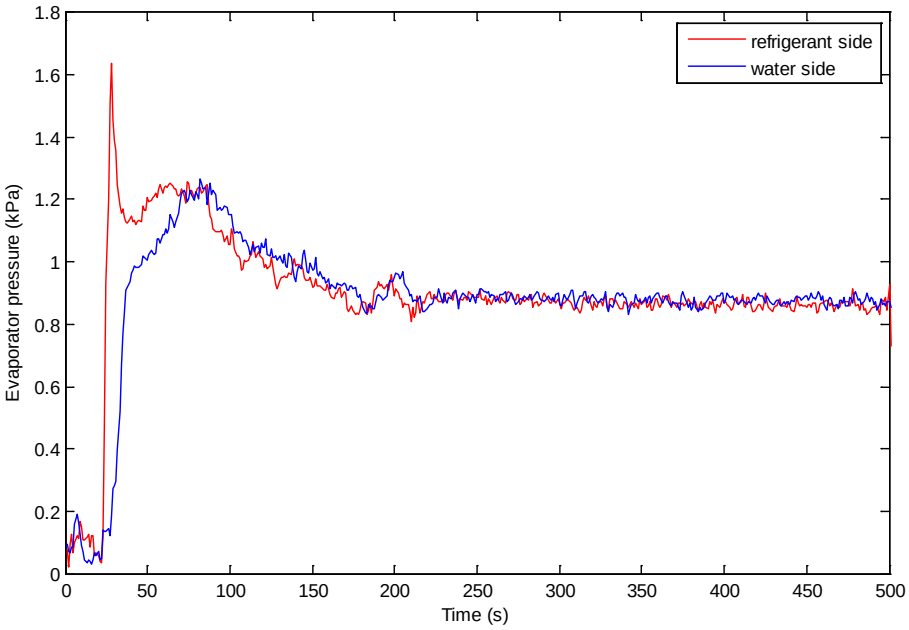

Figure 4.4: Comparison of cooling from water side calculations to refrigerant side calculation

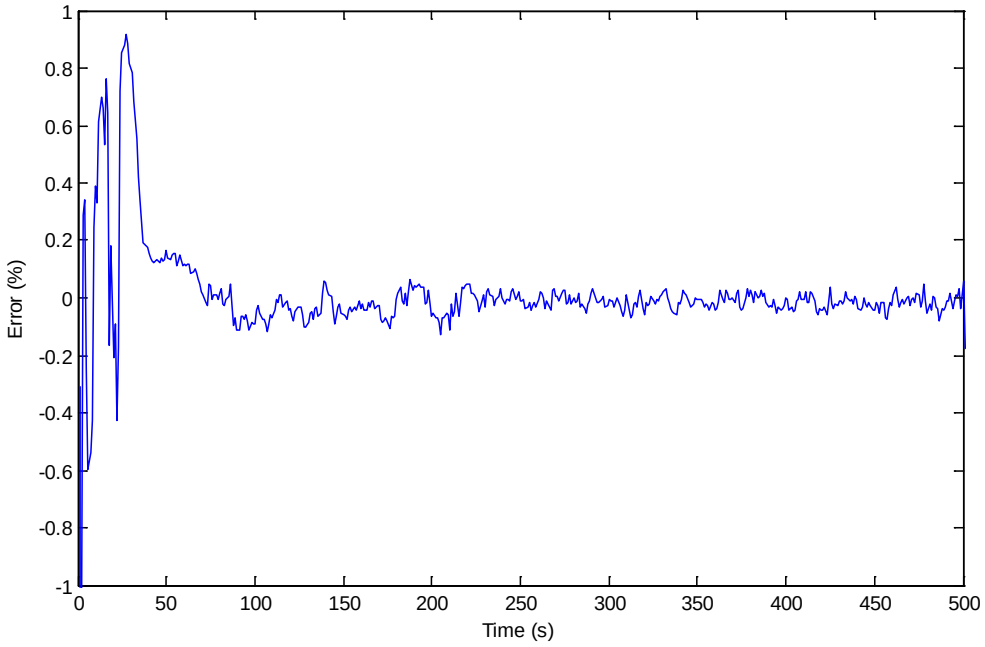

Figure 4.5: Transient differences in energy balances

The recursive least squares algorithm, as discussed earlier is perfectly suited for solving for coefficients of an equation in real time. In this research it is used to develop and update the coefficients of a cost function which is to be minimized to find optimal set-points or optimal operating conditions which will drive the system towards a state of minimum energy consumption.

The Inverse Coefficient of Performance (ICOP) is the cost function, and it is formulated as a function of evaporator pressure and condenser pressure. The ICOP is the total power consumed by the total cooling done by the evaporators. So,

$$\mathrm{ICOP} = \frac{\dot{W}_{\mathrm{total}}}{\dot{Q}_{\mathrm{total}}} \tag{23}$$

The ICOP is formulated from the measurements of evaporator pressure (P_{ero}) and condenser pressure (P_{cro}), which are fit to a polynomial of the form:

$$\mathrm{ICOP} = a_1 + a_2 P_{ero} + a_3 P_{cro} + a_4 P_{ero} P_{cro} + a_5 {P_{ero}}^2 + a_6 {P_{cro}}^2 \tag{24}$$

The formulation of this polynomial thus gives us a data driven model of one aspect of the vapor compression cycle, namely, power consumption. The inverse COP is used instead of minimizing power because the objective of this work is to increase the efficiency of the system without compromising on cooling or power consumption. If only power is used as the cost function, it can be minimized, but at the cost of cooling capacity. The system will seek to minimize the power consumption regardless of decrease in cooling. If only cooling is used in the cost function, the algorithm will seek to maximize cooling at the cost of increased power consumption. The next step would be

to validate this model, and to see how well it tracks the actual measurements for any change in operating conditions. Figure 26 displays the ICOP predicted by the recursive least squares model as opposed to ICOP determined from power and cooling measurements for an experimental run. The system was started and walked through a range of operating conditions to see how the model performed. The ICOP predicted by the algorithm was equal to the average ICOP calculated from the power and cooling measurements as shown in the figure below.

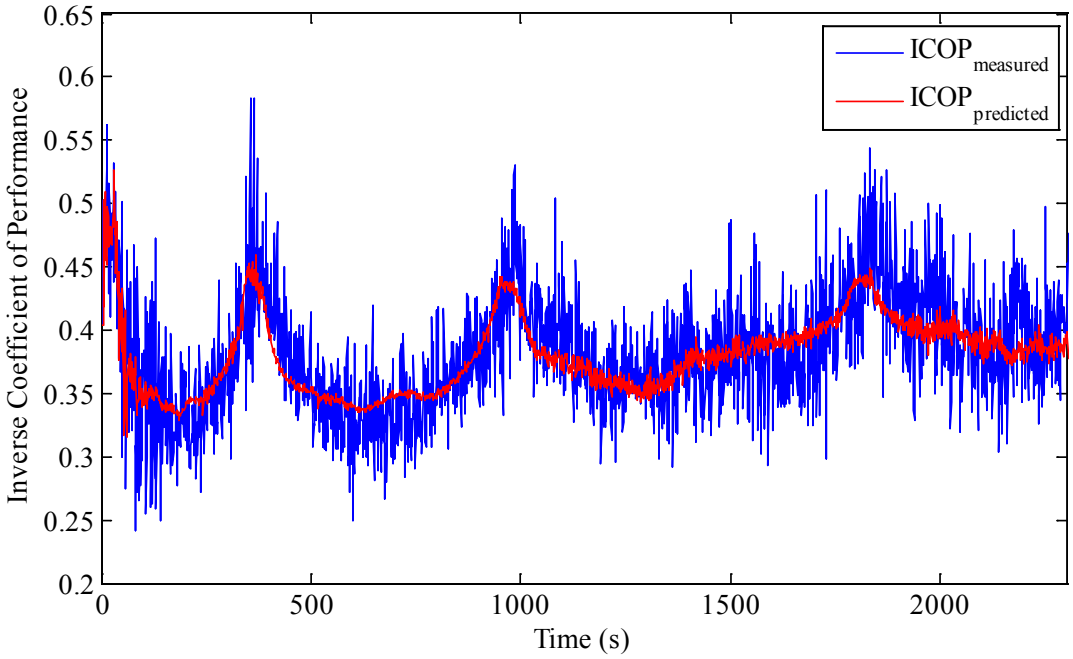

Figure 4.6: ICOP measured compared to ICOP predicted

The error in measured values and predicted values for the ICOP in the test run is about +/- 10% as shown in Figure 4.6. This proves that the ICOP can be accurately predicted using the recursive least squares algorithm.

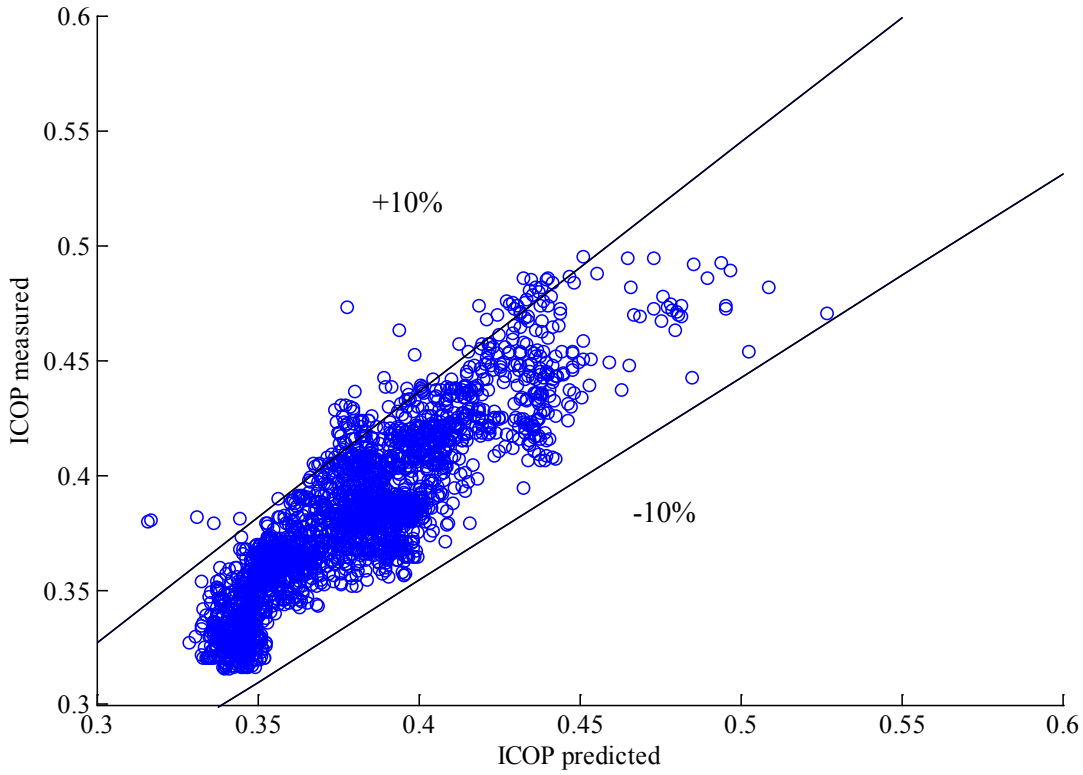

Figure 4.7: Percentage error between ICOP measured and ICOP predicted

The values for P_{ero} and P_{cro} for which the ICOP function is minimum are found by solving the following equations:

$$\frac{dICOP}{dP_{cro}} = 0 \tag{25}$$

$$\frac{dICOP}{dP_{ero}} = 0 \tag{26}$$

These setpoints are then fed to PID controllers that regulate compressor speed and condenser water pump speed to track the setpoints in real time. Another set of controllers are used to maintain the superheat at a desired level and regulate the temperature of

water exiting the evaporator. The actuators used for these actions are the EEV's and the evaporator water pumps respectively.

A low pass filter of the form shown in equations (27) and (28) is included in the algorithm $Pero_{solution}$ and $Pcro_{solution}$ are obtained by solving equations (25) and (26). This introduces a weight 'α' (α=0.01) to the setpoint generated by the algorithm. A small α reduces the difference between two consecutive inputs to the controllers, causing the controllers to track the setpoints gradually, and thus minimizing the effect of unwanted oscillations in setpoints and noise.

$$\mathrm{Pero}_{\mathrm{setpoint}}(\mathrm{k}) = \alpha \mathrm{Pero}_{\mathrm{solution}}(\mathrm{k}) + (1-\alpha)\mathrm{Pero}_{\mathrm{measured}}(\mathrm{k}-1) \quad (27)$$

$$\mathrm{Pcro}_{\mathrm{setpoint}}(\mathrm{k}) = \alpha \mathrm{Pcro}_{\mathrm{solution}}(\mathrm{k}) + (1-\alpha)\mathrm{Pcro}_{\mathrm{measured}}(\mathrm{k}-1) \quad (28)$$

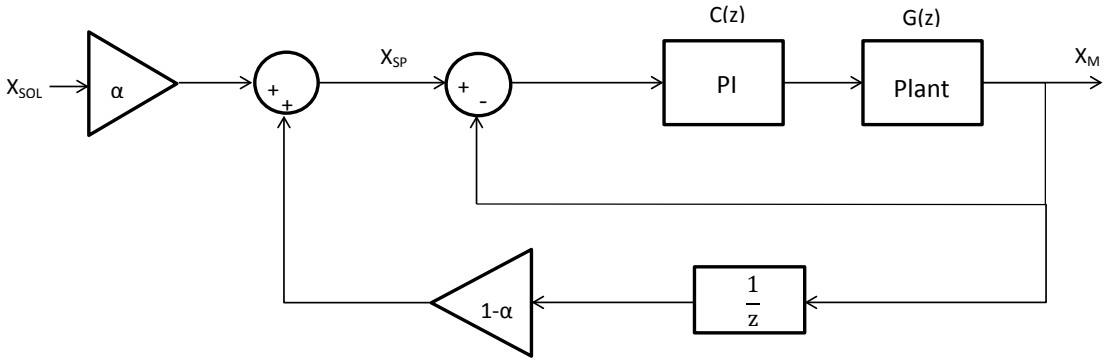

Figure 4.8: Block diagram of plant with filter

Figure 4.8 represents the block diagram of the plant with the controller and filter. The solution to equations 25 and 26 is multiplied by a gain α and summed with the measured value of pressure multiplied by a gain 1-α . the inner loop is the negative feedback of the

PI controller, and the outer loop represents the filter. The loop transfer gain function for the inner loop is given by equation (29)

$$\frac{X_m}{X_{sp}} = \frac{G(z)C(z)}{1 + G(z)C(z)} \tag{29}$$

For perfect tracking, we have $\frac{X_m}{X_{sp}} = 1$, which means that $\frac{G(z)C(z)}{1+G(z)C(z)} = 1$.

Let $\frac{G(z)C(z)}{1+G(z)C(z)} = P(z)$.

Now writing the transfer function from X_{sol} to X_m, ,

$$X_m = P(z)(\alpha X_{sol} + (1-\alpha)H(z)X_m) \tag{30}$$

$$\frac{X_m}{X_{Sol}} = \frac{\alpha P(z)}{1-(1-\alpha)P(z)H(z)} \tag{31}$$

$$\frac{X_m}{X_{Sol}} = \frac{\alpha P(z)}{1-(1-\alpha)P(z)H(z)} \tag{32}$$

Applying the final value theorem for discrete time systems and giving step input as X_{sol},

$$X_{m,ss} = \lim_{z\to 1}(1-z^{-1})(\frac{\alpha P(z)}{1-(1-\alpha)P(z)H(z)})(\frac{1}{1-z^{-1}}) \tag{33}$$

Since P(z) = 1 and H(z) = 1 as z tends to 1,

$$X_{m,ss} = \frac{\alpha}{1-(1-\alpha)} \tag{34}$$

$$X_{m,ss} = 1 \tag{35}$$

From equation 35, we can see that at steady state, the measured value tracks the solution perfectly.

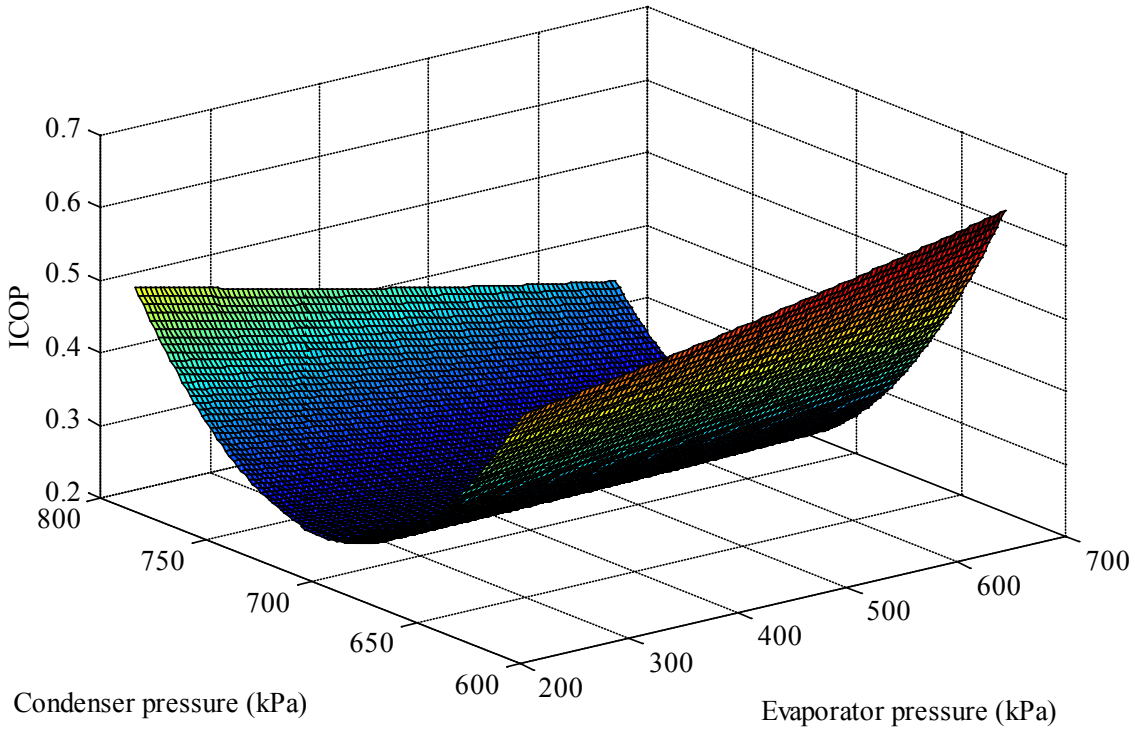

Figure 4.9: 3-D plot showing convexity of ICOP function

The ICOP function is proven to be convex by Larsen in [24]. Tests were run on the multi evaporator system to determine the shape of the curve. The system was run at different operating points, and a surface plot was constructed using the recursive least squares fit for the ICOP function. Figure 4.9 shows a 3 dimensional representation of the ICOP function on the z-axis against evaporator pressure on the x-axis and condenser pressure on the y-axis. The experimental data also suggests that the ICOP function is convex.

The overall control architecture is shown in Figure 4.10:

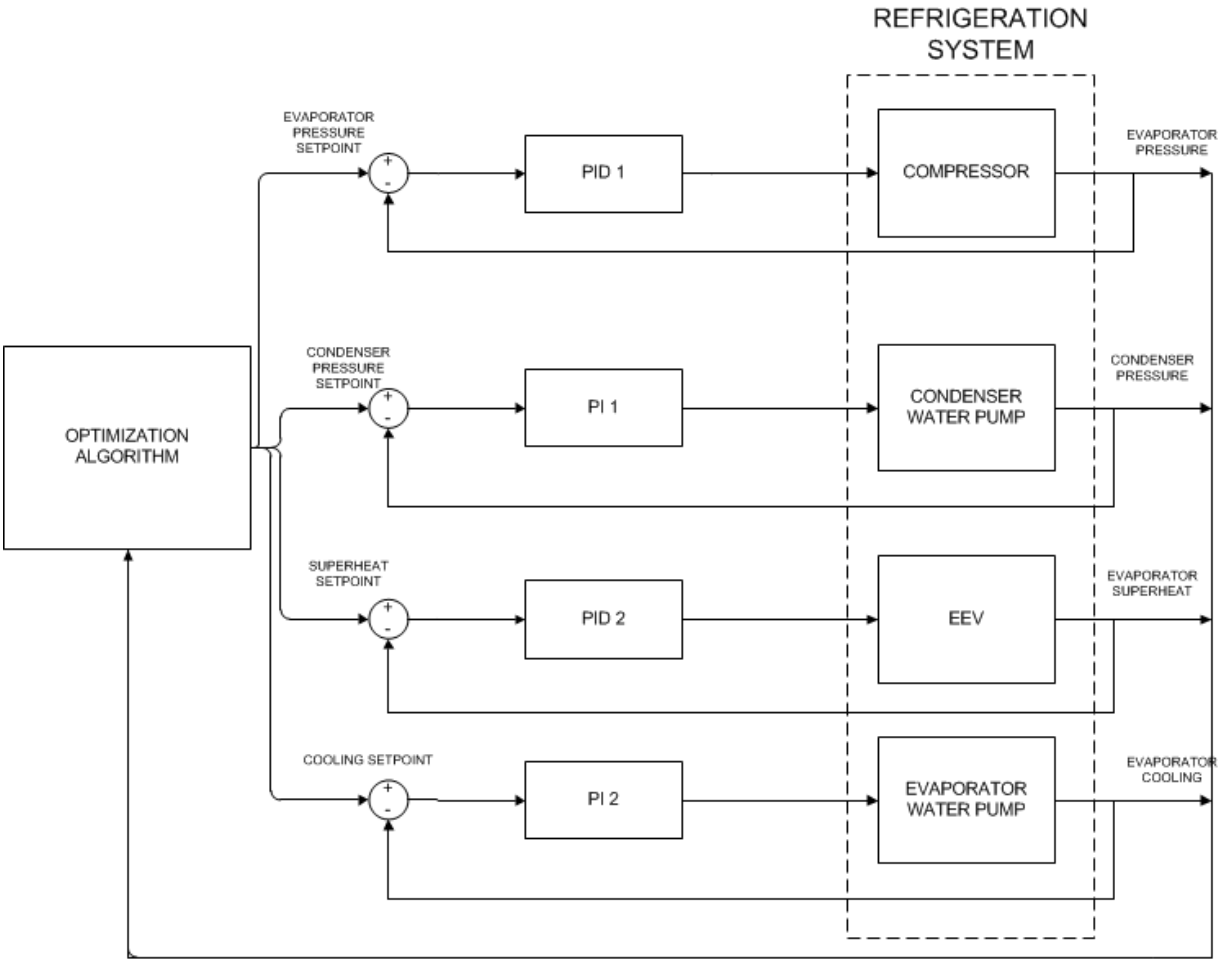

Figure 4.10: Control architecture

CHAPTER V

EXPERIMENTAL VALIDATION OF RECURSIVE LEAST SQUARES ESTIMATION

In this section, the application of the recursive least squares algorithm is discussed. Four test cases are detailed to experimentally validate the working of the theory discussed in the above chapters.

TUNING THE PID CONTROLLERS

PID controllers are used to maintain the operating conditions at desired values. This section discusses the gains for the PID controllers, and setpoint tracking of each input. The results of this test run are shown in the following set of figures. Table 5.1 describes the input-output pairs used and the proportional, differential and integral gains of each controller. Figure 5.1 shows the pressure setpoint tracking of the evaporator. Figure 5.2 shows the condenser pressure setpoint tracking. Figure 5.3 shows the evaporator superheat setpoint tracking, and Figure 5.4 shows the how the water temperature at the outlet of the evaporator is tracked. The table below shows the values of the proportional, integral and differential gains for each of the controllers. Note that when the controllers are added to each of the other two evaporators, the gains remain the same.

Table 5.1: PID controller gains

Controller	Input	Output	K_p	K_i	K_d
PID_1	Compressor	Evaporator Pressure	4	1.2	0.2
PID_2	EEV	Superheat	1.6	0.12	0.05
PI_1	Condenser pump	Condenser Pressure	0.6	0.05	0
PI_2	Evaporator pump	Water temp. at evaporator outlet	0.25	0.05	0

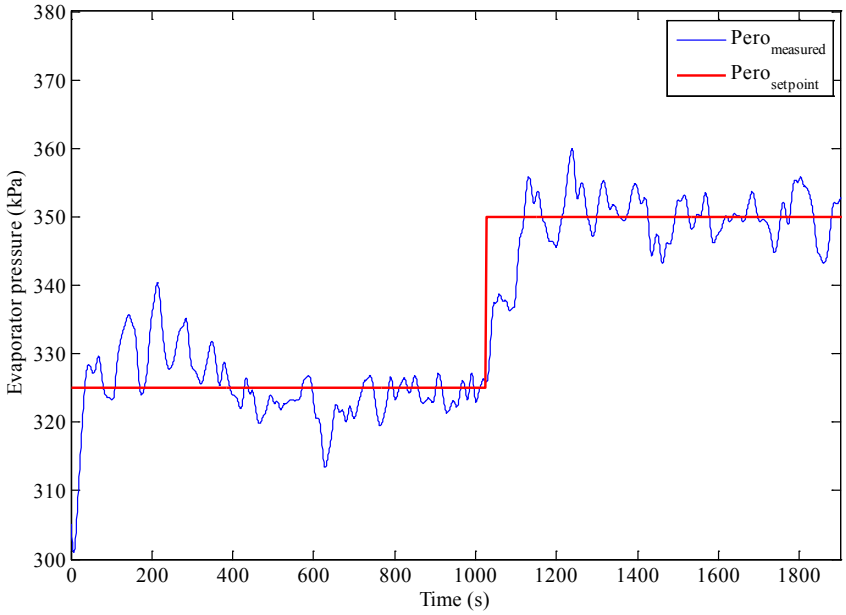

Figure 5.1: Evaporator pressure setpoint tracking

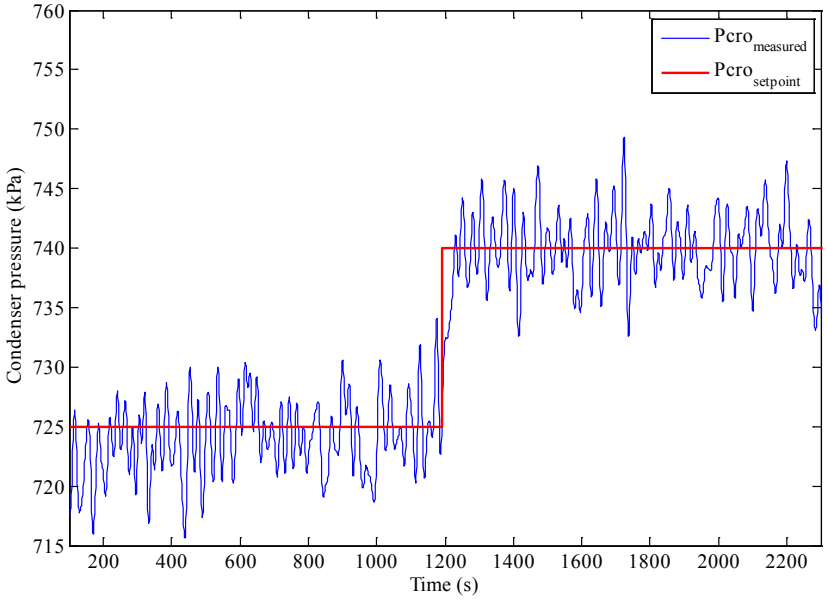

Figure 5.2: Condenser pressure setpoint tracking

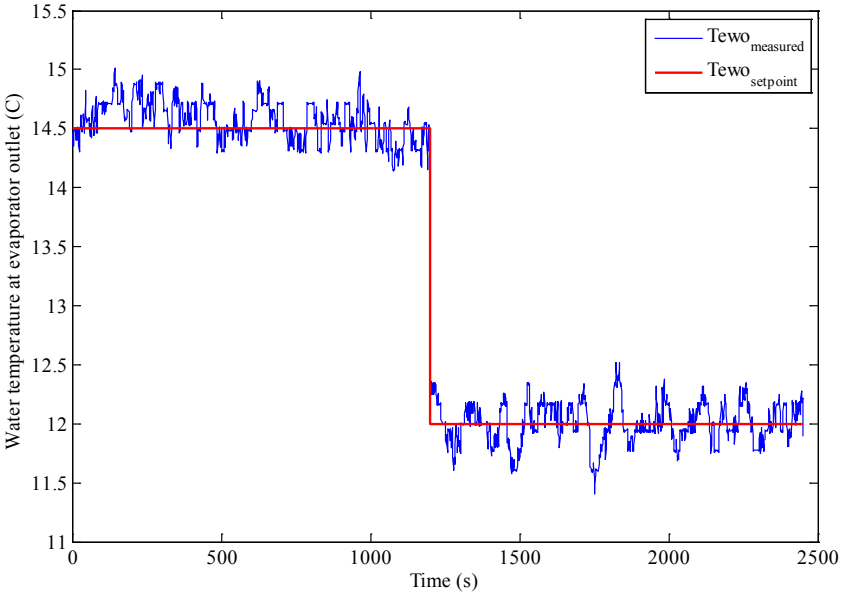

Figure 5.3: Water temperature setpoint tracking

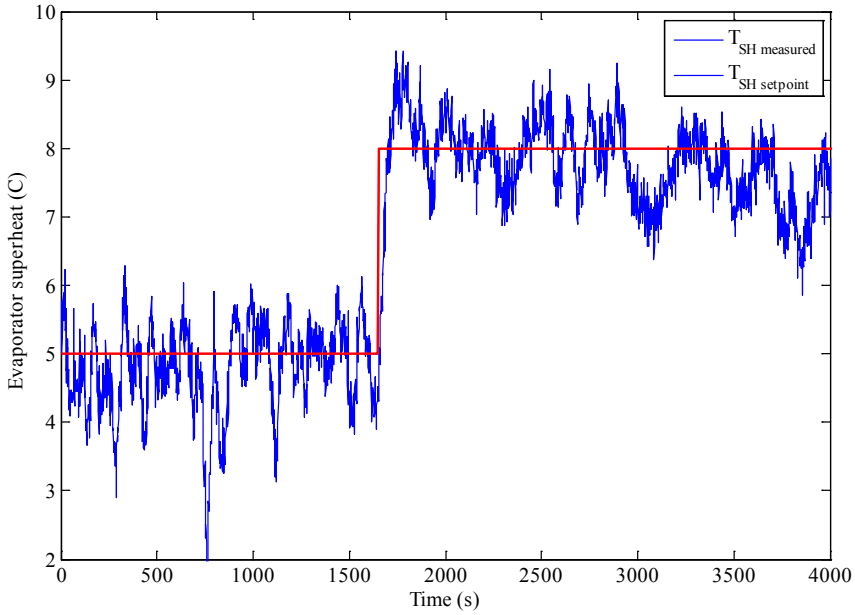

Figure 5.4: Evaporator superheat setpoint tracking

TEST 1: BASE CASE TEST WITH SINGLE EVAPORATOR

The first test will describe the implementation of the recursive least squares algorithm for a single evaporator case. This was chosen as the base case because running a single evaporator offers more flexibility in the sense that various operating conditions can be explored. Firstly, the system was walked through different operating conditions by ramping the compressor speed up every 100 seconds. This was done to gather data to construct a polynomial for the ICOP that is applicable for all operating conditions. As seen from Figures 5.5 and 5.6 below, by ramping up the compressor speed, the evaporator pressure decreases, difference between Evaporating pressures and condensing pressures increases, as a result of which, cooling increases. The first half of the experiment was spent in 'training' the recursive least squares algorithm. Once this was done, the system was brought to a random set of operating conditions which were 325 KPa evaporator pressure and 750 KPa condensing pressure. The system was allowed to settle at these setpoints for some time, at the end of which the controllers were switched on. The evaporator pressure is then increased to about 350 KPa by reducing the compressor speed. The condenser pressure also increases by about 20 KPa to settle at 770KPa. This increase results in a loss of about 0.1 KW of cooling which can be seen in Figure 5.8. The temperature setpoint is maintained at 14 degrees centigrade, even after the controllers are switched on. This is done by reducing the water flow through the evaporator to regulate the water temperature at the outlet of the evaporator.

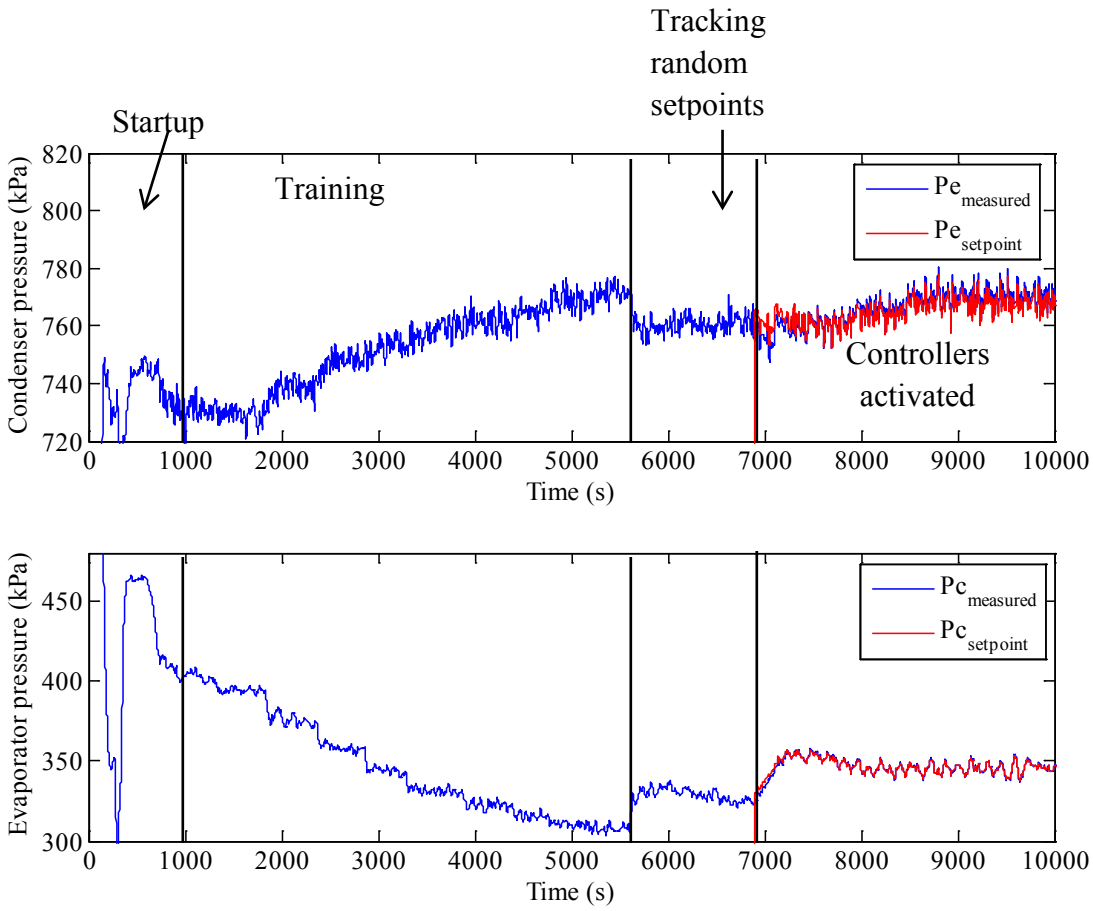

Figure 5.5: Test 1 pressure setpoint tracking

Figure 5.6 below shows the compressor speed being ramped up at regular intervals to provide for the training data set. When the algorithm is switched on shortly after 6000 seconds, the compressor reduces speed to track the evaporator pressure setpoint and settles around 3400 RPM. Figure 5.7 shows the superheat being maintained at 5 degrees centigrade throughout the duration of the test.

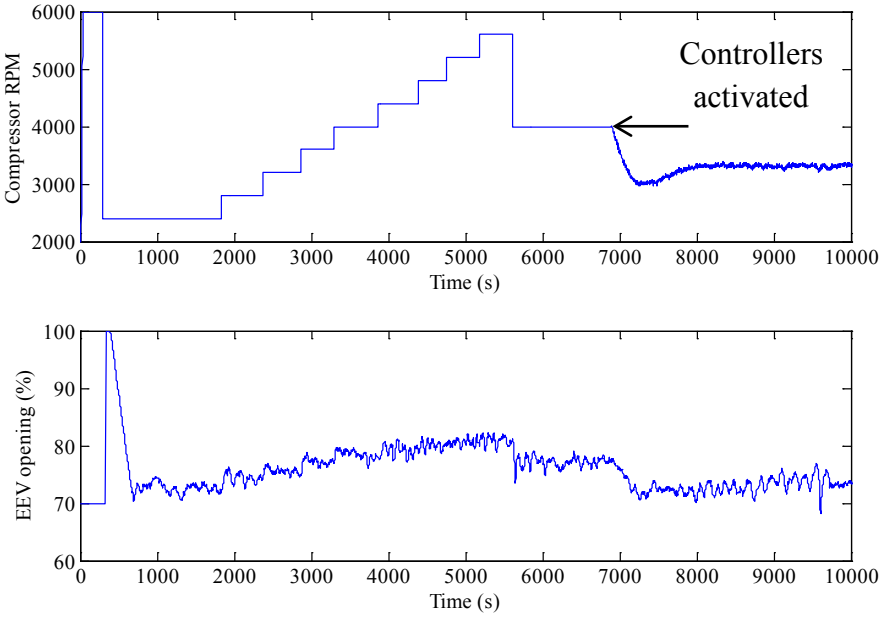

Figure 5.6: Test 1 actuator inputs

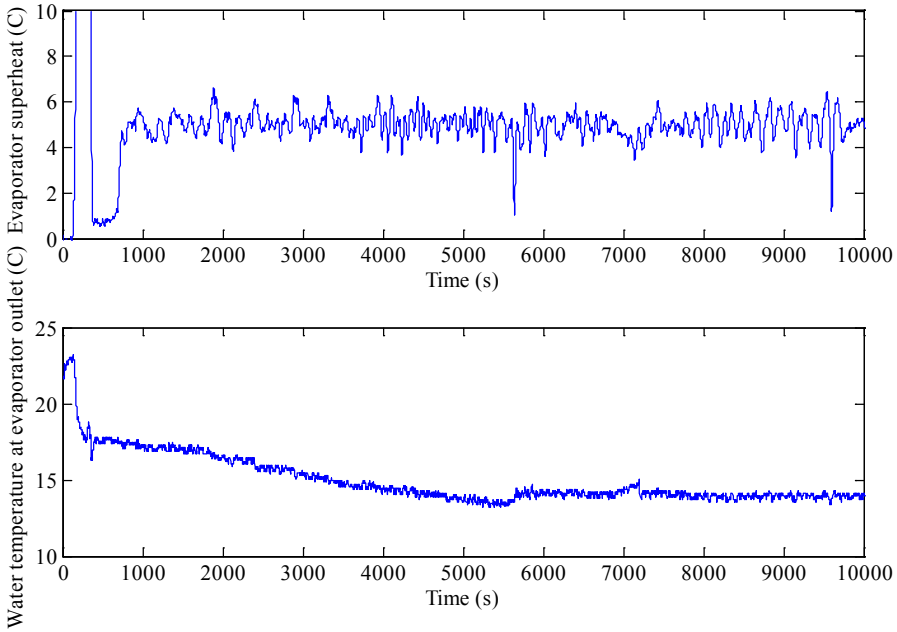

Figure 5.7: Test 1 controlled variables

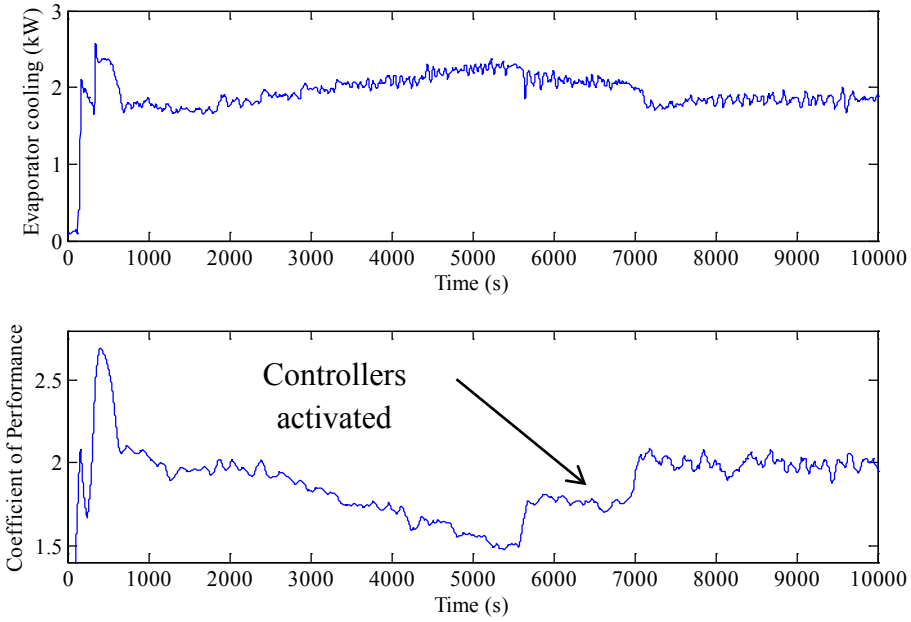

Figure 5.8: Test 1 performance

Figure 5.8 depicts the COP of the system throughout the experiment. The application of the optimal setpoints increases the COP by around 10% (an increase from 1.8 to 2).

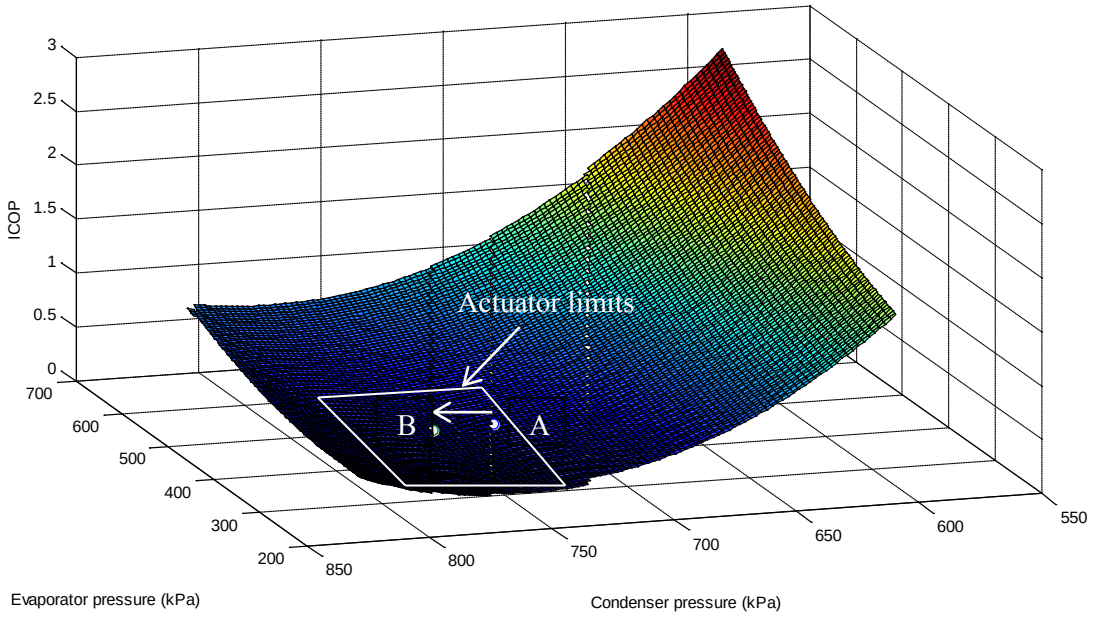

Figure 5.9: Test 1surface plot showing starting and endpoints

TEST 2: SEEKING OPTIMAL SETPOINTS WHILE MAINTAINING CONSTANT COOLING

In the first test, optimal setpoints were attained and decreased the power consumed by the system, but this resulted in a loss in cooling due to the fact that the temperature at the outlet of the evaporator was being regulated. A second test was done to see if the same objectives could be achieved (minimal power consumption), without any loss in cooling. In this test, the evaporator water pump was used to regulate cooling instead of the outlet water temperature. The same procedure as the first test was followed. The system was walked through a range of operating conditions, and then was allowed to come to a steady state condition at randomly chosen evaporator and condenser pressures (300 kPa evaporator pressure and 750 kPa condenser pressure). From here, the input to the

controllers was changed to that provided by the optimizing algorithm. The evaporator pressure increased to 325 kPa and the condenser pressure increased to about 760 kPa (Figure 5.10). This increase in evaporator pressure resulted in a decrease in compressor speed, and ultimately the decrease in power consumed by the compressor. In order to compensate for the decrease in cooling, the water pump speed was increased. Figure 5.11 shows the actuator inputs to the system during the experiment. The Compressor was used to regulate the evaporator pressure and the EEV was used to regulate superheat.

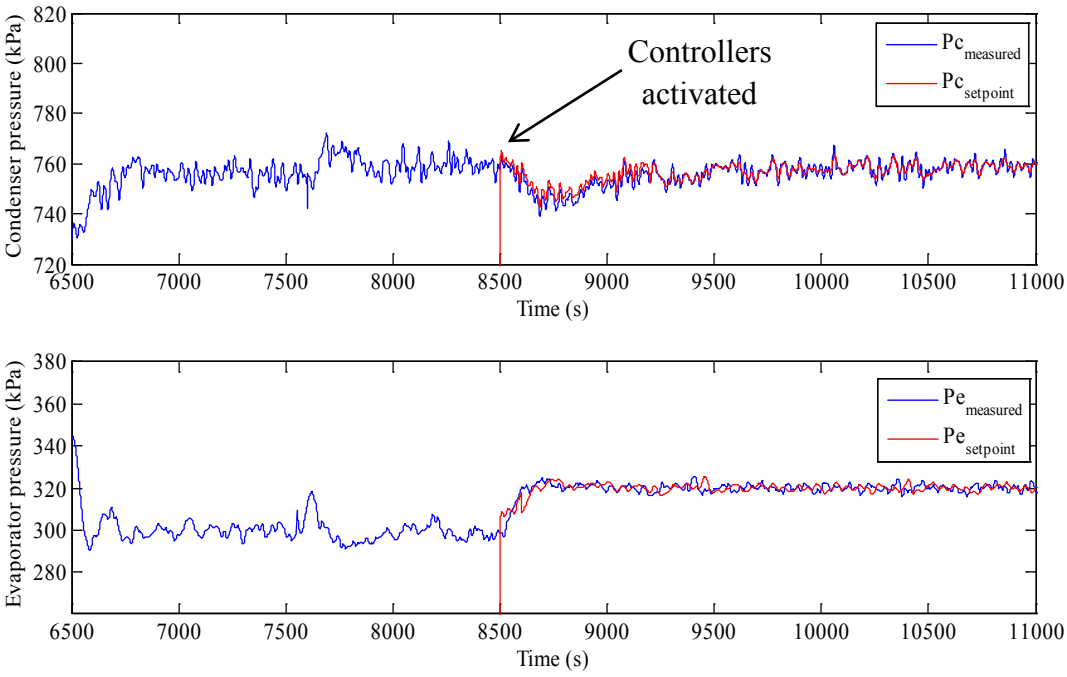

Figure 5.10: Test 2 pressure setpoint tracking

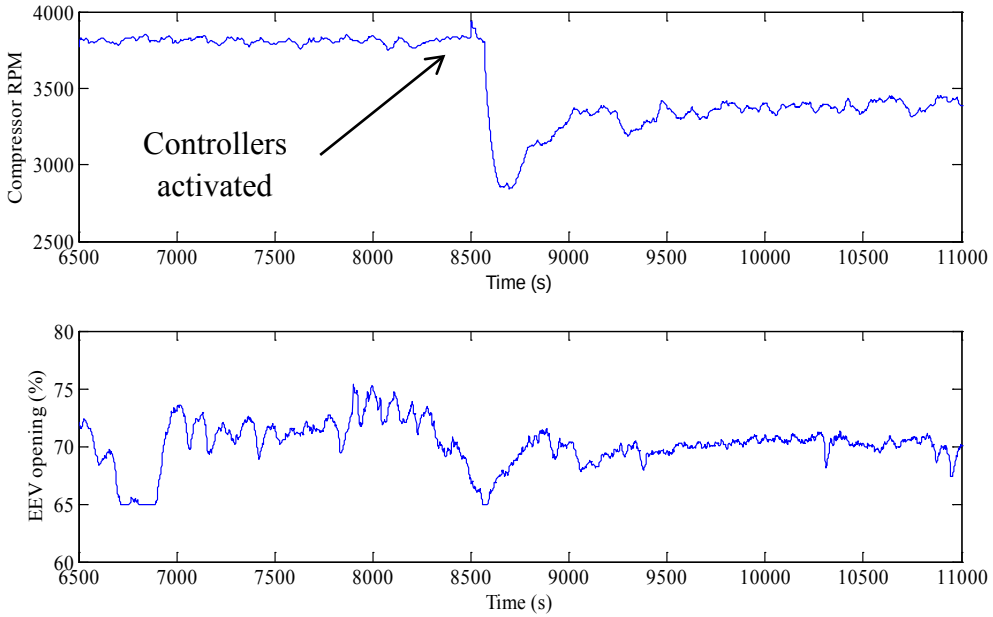

Figure 5.11: Test 2 actuator inputs

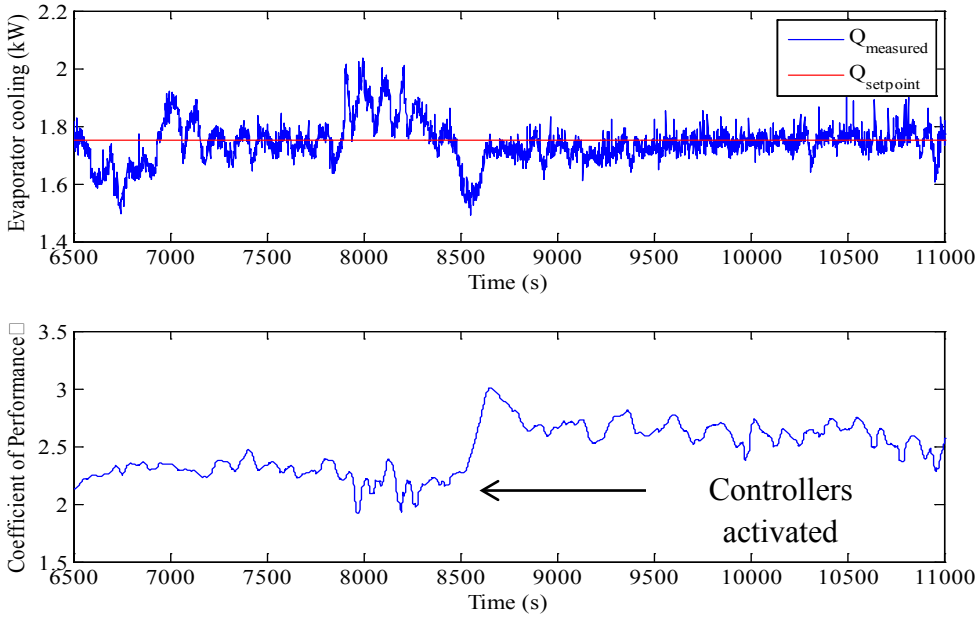

Figure 5.12: Test 2 performance

Figure 5.12 shows the performance measures of the system. The cooling has been maintained at 1.75 kW throughout the experiment. The implementation of the algorithm resulted in an increase is COP from 2.2 to 2.65 (an 18% increase). Figure 5.13 shows a surface plot of the objective function. Point A is the starting point, and point B represents the operating conditions reached after the implantation of the RLS algorithm.

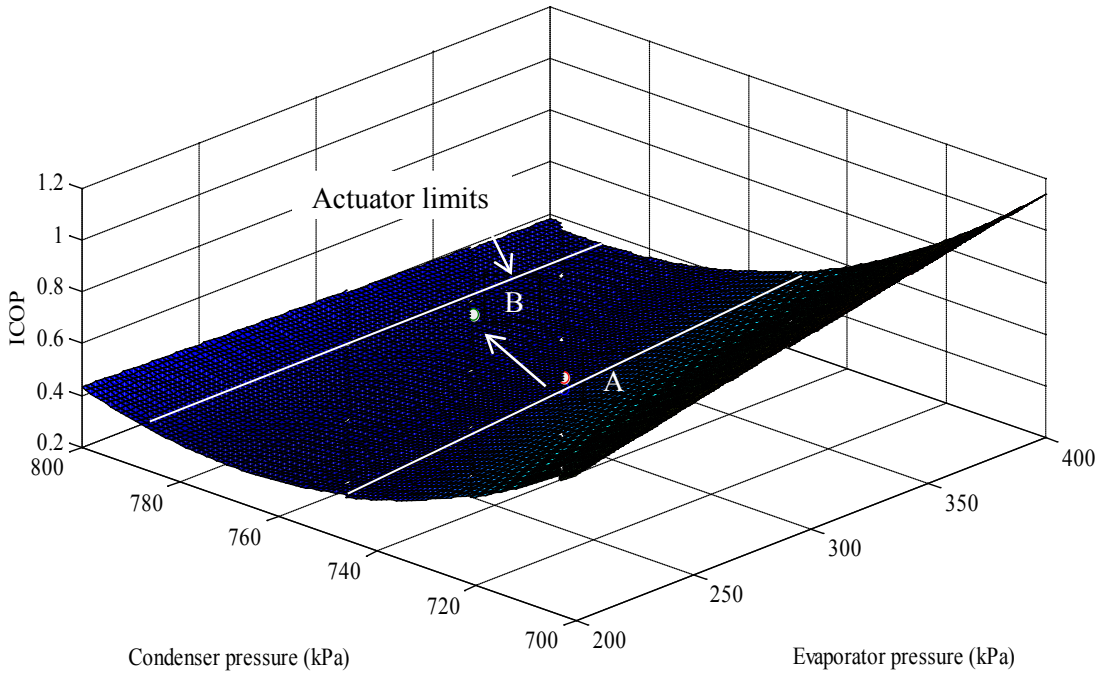

Figure 5.13: Test 2 surface plot showing starting and endpoints

TEST 3: APPLICATION TO MULTIPLE-EVAPORATOR SYSTEM

This case discusses the performance of the algorithm in the case of a multiple evaporator system. The same initial procedure was followed to gather the initial data, this time, with all three evaporators running. Random setpoints were chosen, and the controllers were

set to track them. In this case, the Evaporator pressure was set at 380 KPa and the condensing pressure was set at 725 KPa. The algorithm was implemented as shown in the figures below. This brought about an increase in 10 KPa for the evaporator pressure and 35 KPa for the condenser pressure. The increase in condenser pressure resulted in a corresponding decrease speed of the condenser water pump to reduce water flow as required.

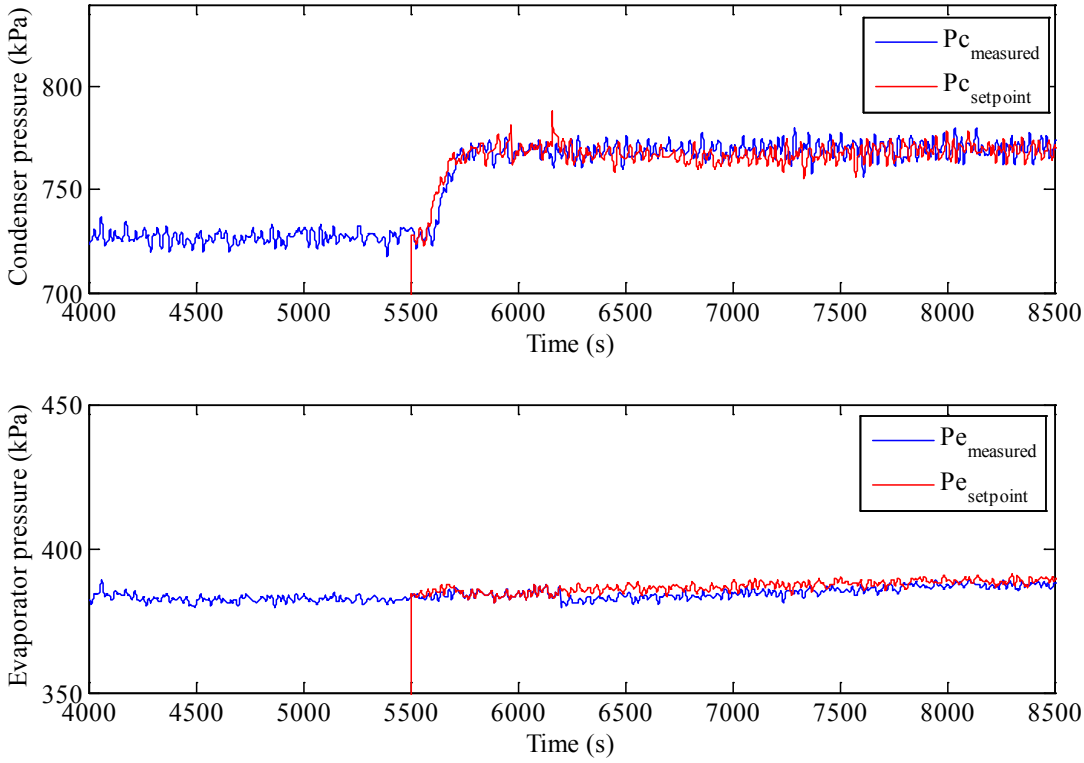

Figure 5.14: Test 3 pressure setpoint tracking

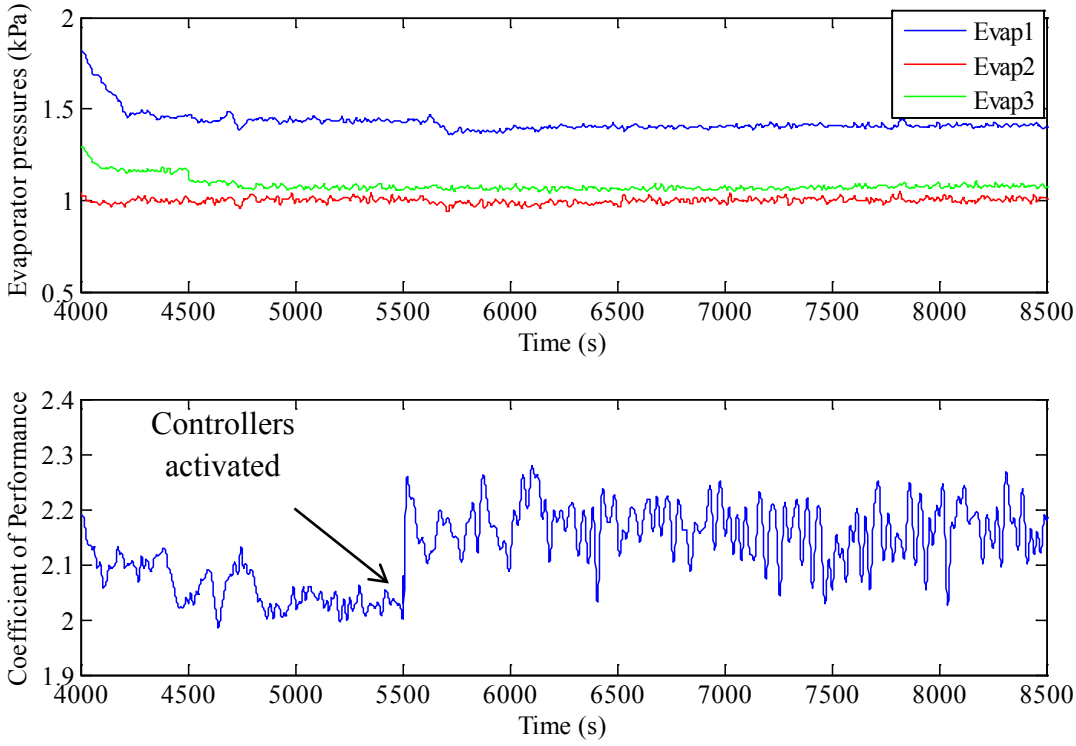

Figure 5.15: Test 3 performance

Figure 5.15 shows that the cooling in each of the three evaporators remains constant after the controllers start tracking the optimal setpoints. The change in COP before and after the implementation of the algorithm is also shown. The COP increases to about 2.15 from 2, which is a 7.5% increase.

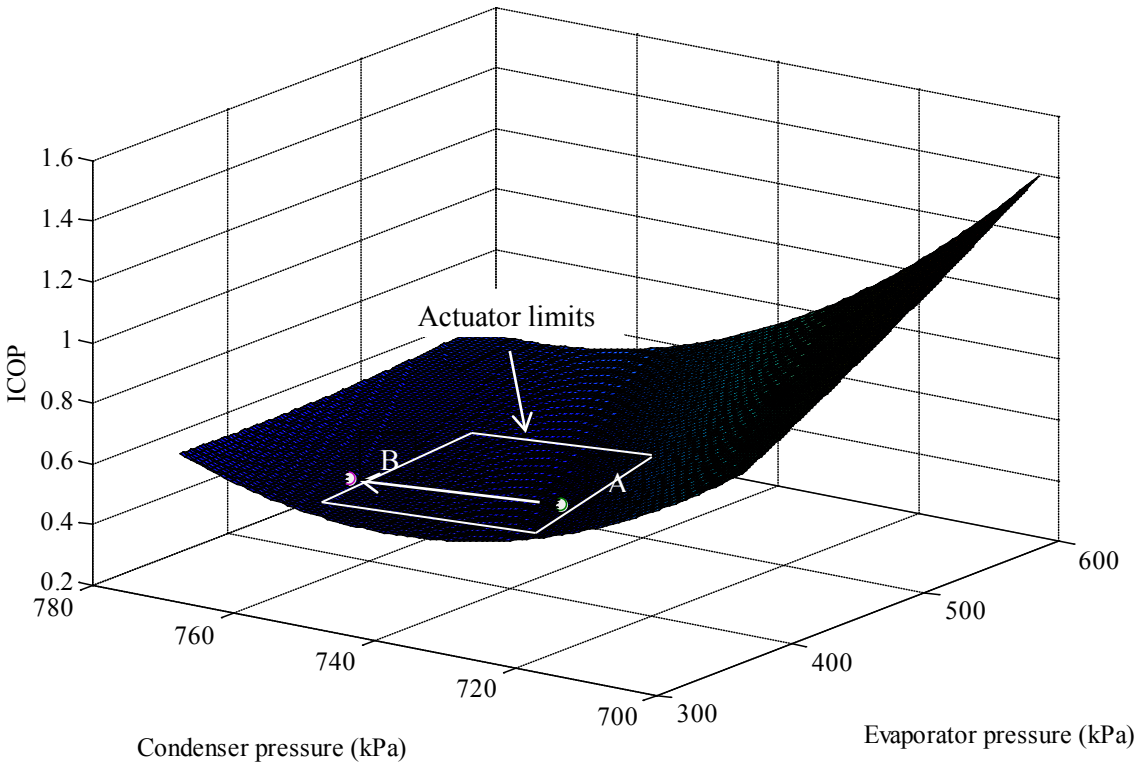

Figure 5.16: Test 3 surface plot showing starting and endpoints

TEST 4: ADAPTABILITY TO CHANGES IN OPERATING CONDITIONS

This test is designed to verify that the algorithm can adapt accordingly to a change in operating conditions caused by a disturbance. There were two experimental runs involved in testing this case. First, the system was started and allowed to come to a steady state. At around 3000 seconds, the speed pumps supplying water to the evaporators was increased which resulted in an increase in temperature of water at the outlet of the evaporator. This action increased the total power consumed by the system. This resulted in a decrease in the COP of the system because more power was being consumed to provide a small increase in cooling.

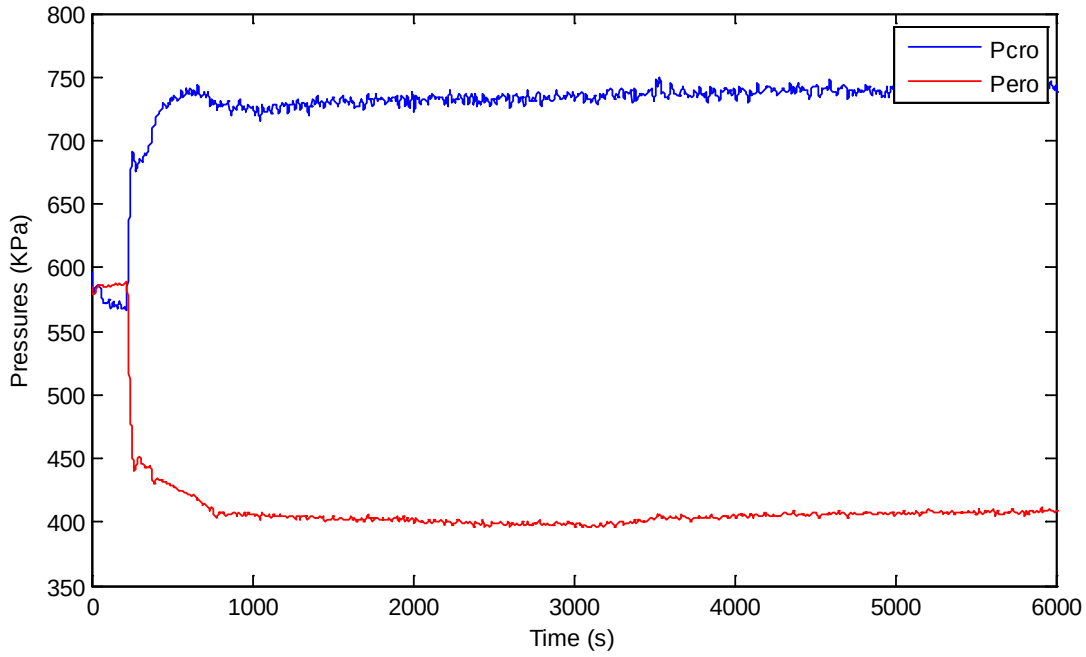

Figure 5.17: Test 4A Evaporator and condenser pressures

Figure 5.18 shows the increase in T_{ewo} by 1 degree centigrade in each of the evaporators as a result of an increase in pump speed.

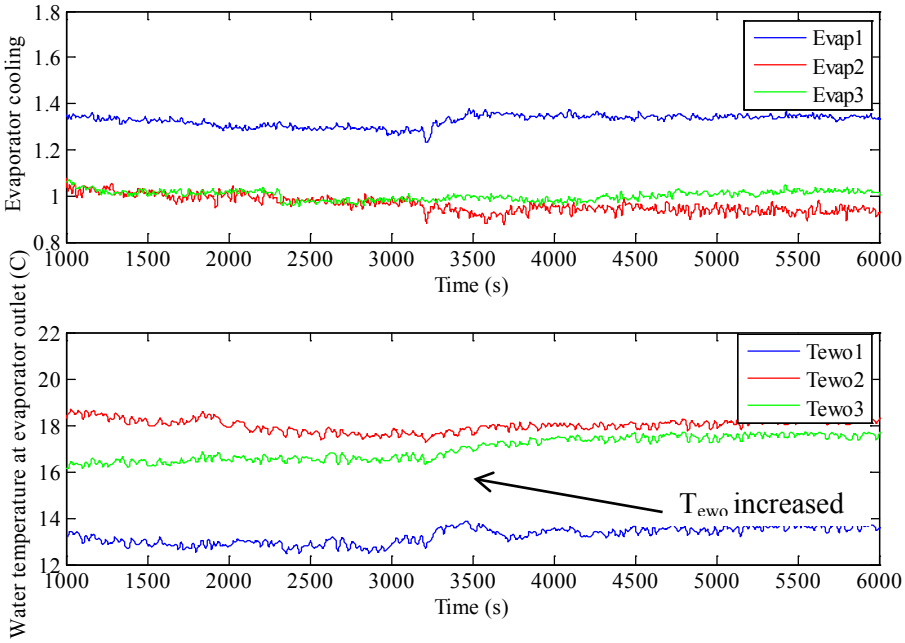

Figure 5.18: Test 4A Evaporator cooling and temperature of water at evaporator outlet

TEST 4B

The same test was run again, this time, with the algorithm being implemented at about 4500 seconds. The fan speeds were increased at 5500 seconds. Figure 5.19 shows the condenser pressure and evaporator pressure setpoints and their tracking. The optimal evaporator pressure was found to be about 20 KPa more than what it was in the previous run, and the condenser pressure was found to be around 780 KPa. Figure 5.20 shows the cooling and water temperatures respectively.

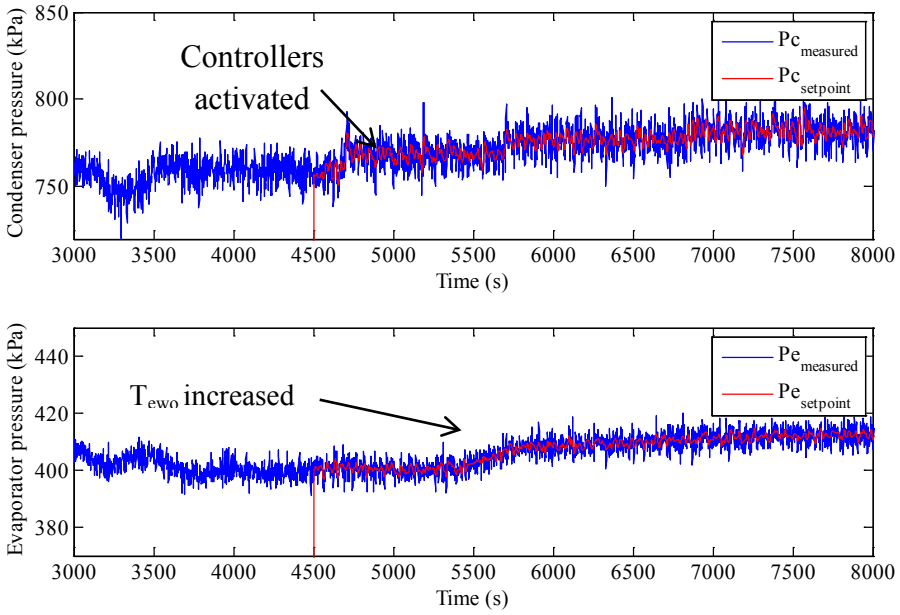

Figure 5.19: Test 4B pressure setpoint tracking

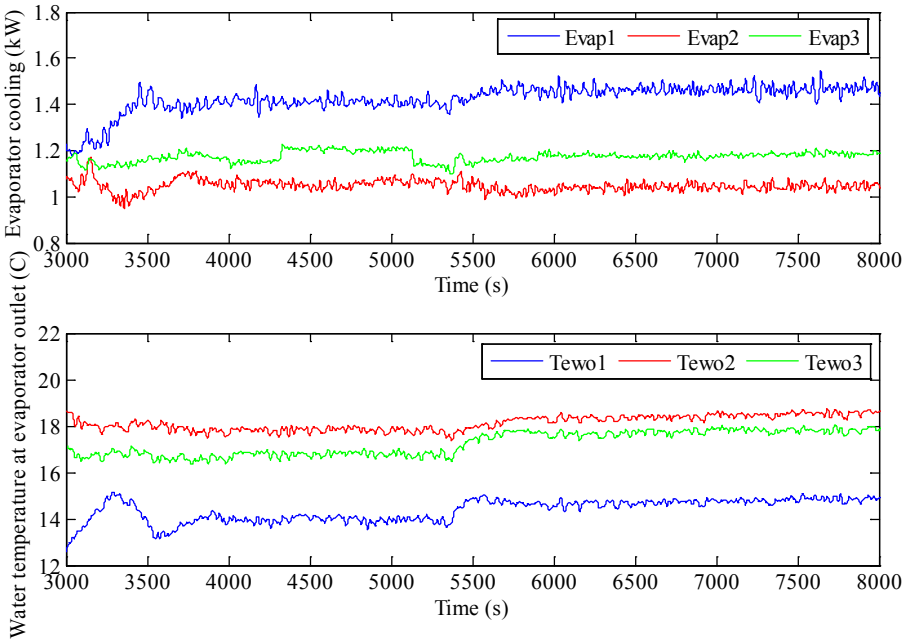

Figure 5.20: Test 4B controlled variables

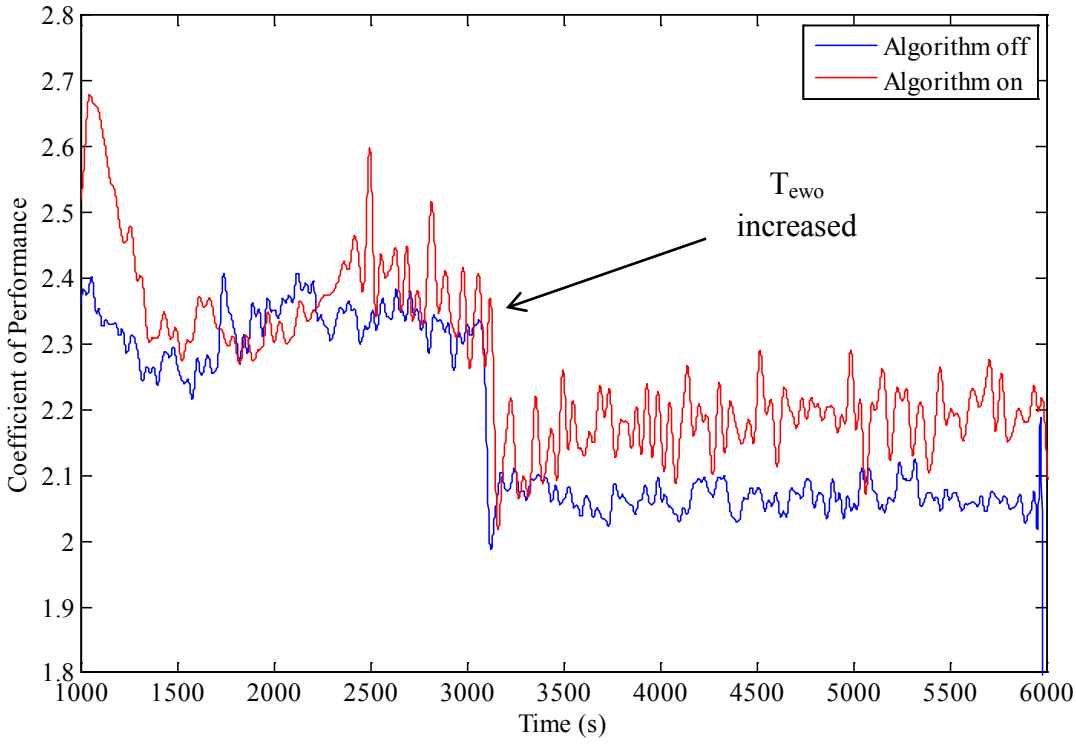

Figure 5.21: Test 4 comparison of COPs for the two runs

Figure 5.21 compares the COPs obtained from the two runs. The COP decreases in both runs, as expected, but the decrease in COP with the implementation of the algorithm was less (7%) compared the previous run. Note that the time scale for the validation run has been adjusted to be able to compare it to the test run.

CHAPTER VI

CONCLUSION

This thesis presents a novel approach that seeks to maximize the coefficient of performance of a vapor compression cycle without using any mathematical models of components and any *a priori* information. This approach presents an algorithm that develops a cost function using a recursive least squares regression approach which is then minimized to obtain optimal set points for evaporator and condenser pressures. These setpoints are then fed to local PID controllers which are used to drive the system to a more efficient operating condition while maintaining temperatures of the cooling zones at desired levels. The control architecture presented was shown to achieve the desired objectives. The major improvement that this thesis presents over conventional data based approaches is the adaptability of the algorithm according to changes in operating conditions.

FUTURE WORK

While the approach presented in this thesis has met the required objectives, there is always room for improvement and further research on the topic. In this section, ideas for future work are discussed.

STABILITY

Stability of any control approach is a fundamental issue that needs to be addressed. In the algorithm presented in this thesis, a low pass filter was used to keep the setpoints to

be fed to the controllers within acceptable limits. Though this method is effective, investigations can be made to determine the stability of the recursive least squares approach itself.

RECURSIVE LEAST SQUARES WITH VARIABLE FORGETTING FACTOR

A forgetting factor is a parameter that is used to determine how much of the previous data is to be used while estimating the regression polynomial by exponentially giving less weight to older samples. Studies can be done to incorporate the use of a variable forgetting factor and its effect on the stability of the approach.

EXPANSION OF APPROACH TO REFRIGERATION SYSTEMS OF DIFFERENT CONFIGURATIONS

It would be interesting to determine whether this approach can be applied to other configurations of vapor compression systems. For example, would it work in the case of multiple compressors, or evaporators connected in series? And if so, how to implement the algorithm to these configurations.

REFERENCES

[1] U.S. Department of Energy. (2001). End use consumption of electricity by end use and appliance. Available: http://www.eia.doe.gov/emeu/recs2001/enduse2001/enduse2001.html

[2] Y. A. B. Çengel, Michael A., *Thermodynamics :An Engineering Approach*, 4th ed. Boston: McGraw-Hill, 2005.

[3] R. Shah, A. G. Alleyne, C. W. Bullard, B. P. Rasmussen, and P. S. Hrnjak, "Dynamic modeling and control of single and multi-evaporator subcritical vapor compression systems,". University of Illinois at Urbana-Champaign., 2003.

[4] S. Wang and Z. Ma, "Supervisory and optimal control of building hvac systems: a review," *HVAC&R Research,* vol. 14, pp. 3-32, 2008.

[5] W. D. Gruhle and R. Isermann, "Modeling and control of a refrigerant evaporator," in *American Control Conference*, 1985, pp. 287-292.

[6] A. Outtagarts, P. Haberschill, and M. Lallemand, "The transient response of an evaporator fed through an electronic expansion valve," *International Journal of Energy Research,* vol. 21, pp. 793-807, 1997.

[7] D. P. Finn and C. J. Doyle, Control and Optimization Issues Associated with Algorithm-Controlled Refrigerant Throttling Devices, *ASHRAE Transactions*, vol. 106,pp. 524-533, Jul. 2000.

[8] H. Rasmussen, C. Thybo, and L. F. S. Larsen, "Nonlinear superheat and evaporation temperature control of a refrigeration plant," in *Proc. 2006 IFAC Workshop on Energy Saving Control in Plants and Buildings*, Bansko, Bulgaria, Oct. 2006, pp. 251-254..

[9] M. S. Elliott and B. P. Rasmussen, "A model-based predictive supervisory controller for multi-evaporator HVAC systems," in *American Control Conference, 2009. ACC '09.*, 2009, pp. 3669-3674.

[10] X.-D. He, S. Liu, and H. H. Asada, "Modeling of vapor compression cycles for multivariable feedback control of hvac systems," *Journal of Dynamic Systems, Measurement, and Control,* vol. 119, pp. 183-191, 1997.

[11] X.-D. He, S. Liu, H. H. Asada, and H. Itoh, "Multivariable control of vapor compression systems," *HVAC&R Research,* vol. 4, pp. 205-230, 1998/07/01 1998.

[12] H. Xiang-Dong and H. H. Asada, "A new feedback linearization approach to advanced control of multi-unit HVAC systems," *American Control Conference, 2003. Proceedings of the 2003*, 2003, vol.3, pp. 2311-2316.

[13] L. S. Larsen, "Control methods utilizing energy optimizing schemes in refrigeration systems," in *Proc of European Controls Conference 2003*, September 2003.

[14] J. Sun and A. Reddy, "Optimal control of building HVAC&R systems using complete simulation-based sequential quadratic programming (CSB-SQP)," *Building and Environment,* vol. 40, pp. 657-669, 2005.

[15] Y. Yao, "Optimal operation of a large cooling system based on an empirical model," *Applied Thermal Engineering,* vol. 24, p. 2303, 2004.

[16] B. C. Ahn, "Optimal control development for chilled water plants using a quadratic representation," *Energy and Buildings,* vol. 33, p. 371, 2001.

[17] S. B. Austin, "Chilled water system optimization," *ASHRAE Journal Vol: 35,no:7,* pp. 50-56; 1993.

[18] L. Lu, "Global optimization for overall HVAC systems—Part I problem formulation and analysis," *Energy Conversion and Management,* vol. 46, p. 999, 2005.

[19] R. T. Olson and J. S. Liebman, "Optimization of a chilled water plant using sequential quadratic programming," *Engineering Optimization,* vol. 15, pp. 171-191, 1990.

[20] Mathworks Inc. 2012. System Identification Toolbox Manual. Available: http://www.mathworks.com/products/sysid/

[21] P. Van Overschee and B. De Moor, "N4SID: Subspace algorithms for the identification of combined deterministic-stochastic systems," *Automatica,* vol. 30, pp. 75-93, 1994.

[22] L. Ljung, "System Identification," in *Wiley Encyclopedia of Electrical and Electronics Engineering*, 2nd ed, Upper Saddle River,NJ, John Wiley & Sons, Inc., 2001.

[23] S. L. John M. Lewis and S. Dhall, *Recursive Least Squares Estimation Dynamic Data Assimilation*:, Cambridge, Cambridge University Press, 2006.

[24] L. F. S. Larsen, *Model based control of refrigeration systems*, Nordborg, Denmark, AAlborg University, 2006.